

008

GEORGIA INSTITUTE OF TECHNOLOGY
OFFICE OF CONTRACT ADMINISTRATION
SPONSORED PROJECT INITIATION

Date: July 23, 1976

Project Title: An Investigation of the Effects of Frequency Agility on the Correlation Properties of Land Clutter and Targets

Project No: A-1858

Project Director: Mr. E. E. Martin

Sponsor: Massachusetts Institute of Technology; Lincoln Lab., Lexington, Mass
02173

Agreement Period: From June 10, 1976 Until Sept. 30, 1976 (Contr. Exp.

Type Agreement: P.O. # CX-1069 (subcontract under F19628-76-C-0002)

Amount: \$30,000

Reports Required: Monthly Technical Reports; Monthly Fiscal Reports; Final Report

Sponsor Contact Person (s):

Technical Matters

Dr. Joseph L. Katz
Engineer-in-Charge

Contractual Matters

(thru OCA)
C. W. Cahalane
Associate Purchase Agent

Massachusetts Institute of Technology
Lincoln Laboratory
P.O. Box 73
Lexington, Massachusetts 02173
(617) 862-5500

Defense Priority Rating: DO-A7 under DMS Reg. 1

Assigned to: Applied Engineering ~~(School/Laboratory)~~

COPIES TO:

Project Director
Division Chief (EES)
School/Laboratory Director
Dean/Director-EES
Accounting Office
Procurement Office
Security Coordinator (OCA)
Reports Coordinator (OCA)

Library, Technical Reports Section
Office of Computing Services
Director, Physical Plant
EES Information Office
Project File (OCA)
Project Code (GTRI)
Other

GEORGIA INSTITUTE OF TECHNOLOGY
OFFICE OF CONTRACT ADMINISTRATION

SPONSORED PROJECT TERMINATION

Date: May 24, 1977

Project Title: An Investigation of the Effects of Frequency Agility on the
Correlation Properties of Land Clutter and Targets

Project No: A-1858

Project Director: Mr. E. E. Martin

Sponsor: Massachusetts Institute of Technology; Lincoln Lab., Lexington, Mass. 02173

Effective Termination Date: 11/15/76 (Contract Expiration)

Clearance of Accounting Charges: 11/30/76

Grant/Contract Closeout Actions Remaining:

☒ Final Invoice and Closing Documents

☐ Final Fiscal Report

☒ Final Report of Inventions

☒ Govt. Property Inventory & Related Certificate *← requested 31 May '77*

☒ Classified Material Certificate

☐ Other _____

Assigned to: Radar Instrumentations Laboratory (School/Laboratory)

COPIES TO:

Project Director
Division Chief (EES)
School/Laboratory Director
Dean/Director-EES
Accounting Office
Procurement Office
Security Coordinator (OCA) ✓
Reports Coordinator (OCA)

Library, Technical Reports Section
Office of Computing Services
Director, Physical Plant
EES Information Office
Project File (OCA)
Project Code (GTRI)
Other _____

A-1858



ENGINEERING EXPERIMENT STATION

GEORGIA INSTITUTE OF TECHNOLOGY • ATLANTA, GEORGIA 30332

19 July 1976

Massachusetts Institute of Technology
Lincoln Laboratory
Lexington, Massachusetts 02173

ATTN: Dr. Joseph Katz

RE: Purchase Order No. CX-1069

SUBJECT: Project Status Report No. 1

Gentlemen:

A summary of the technical progress for the period 10 June 1976 through 30 June 1976 on the referenced contract is contained herein.

For administrative purposes this program has been assigned to the Radar Technology Division under the direction of Mr. J. L. Eaves. Mr. E. E. Martin will serve as project director and will be responsible for overall project management and for the collection and analysis of the data under Task I of the proposal. Mr. N. C. Currie will serve as associate project director and will be responsible for the analysis of the Winter Foliage Penetration Data under Task II of the proposal.

Technical Progress

Modifications to the data collection radar were begun immediately upon notification of contract award. A review of the data requirements called for in the Addendum to Proposal revealed that a more extensive modification of the radar was required than initially had been anticipated. However, fabrication of all new circuit cards has been accomplished, and work on the installation of these circuits in the video processor is 70 per cent complete. The microwave assembly of the radar has been installed in the radar van, and preliminary evaluation and test of the rf/af portion of the radar has been completed.

Future Efforts

Installation of the additional circuits is expected to be completed by 7 July 1976 and testing of the complete radar system will begin at that time. These tests will be conducted on the Georgia Tech campus and should be completed by 16 July 1976. At present, two measurement sites are under

Massachusetts Institute of Technology
Monthly Progress Report No. 1
Page 2
19 July 1976

consideration. One site is located at Pine Mountain, near Warm Springs, Georgia, and the other site is located at Stone Mountain, near Atlanta. The final selection of the measurement site is dependent on the availability of private land for the location of the vehicle target. The local Marine Reserve and the Georgia National Guard are being contacted in an effort to obtain a vehicle for these tests. It is expected that a vehicle can be obtained as soon as specific dates for the field operations are determined.

Respectfully submitted,

E. E. Martin
Project Director

cc: A-1858 file
JLEaves
FBDyer
HAEcker
NCCurrie

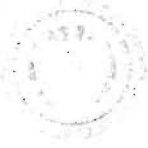
Approved:

J. L. Eaves
Chief, Radar Technology Division

TASK MILESTONE CHART Project A-1858

[illegible]

A-1858



ENGINEERING EXPERIMENT STATION

GEORGIA INSTITUTE OF TECHNOLOGY • ATLANTA, GEORGIA 30332

29 July 1976

Massachusetts Institute of Technology
Lincoln Laboratory
Lexington, Massachusetts 02173

ATTENTION: C. W. Cahalane

REFERENCE: Purchase Order No. CX1069

SUBJECT: Monthly Fiscal Status Report No. 1

Gentlemen:

A summary of the fiscal status of the referenced contract purchase order covering the period 10 June 1976 through 30 June 1976 is contained herein.

	<u>Month</u>	<u>Total to Date</u>
Engineering man-hours expended	176	176
Total man-hours expended	176	176
Funds Expended	\$2,855	\$2,855
Estimated fiscal material commitment	\$ 14	\$ 14

It is anticipated that work under this contract will be completed within the contract commitment.

Respectfully submitted,

E. E. Martin
Project Director

EEM/nlj

cc: J. L. Eaves

A-1858



ENGINEERING EXPERIMENT STATION
GEORGIA INSTITUTE OF TECHNOLOGY • ATLANTA, GEORGIA 30332

6 August 1976

Massachusetts Institute of Technology
Lincoln Laboratory
Lexington, Massachusetts 02173

ATTENTION: C. W. Cahalane

REFERENCE: Purchase Order No. CX1069

SUBJECT: Monthly Fiscal Status Report No. 2

Gentlemen:

A summary of the fiscal status of the referenced contract purchase order covering the period 1 July 1976 through 31 July 1976 is contained herein.

	<u>Month</u>	<u>Total to Date</u>
Engineering man-hours expended	239	415
Total man-hours expended	251	427
Funds Expended	\$3,796.	\$6,651.
Estimated fiscal material commitment	\$ 264.	\$ 278.

It is anticipated that work under this contract will be completed within the contract commitment.

Respectfully submitted,

E. E. Martin
Project Director

Approved:

J. L. *[Signature]* Eaves, chief, Radar Technology Division



ENGINEERING EXPERIMENT STATION

GEORGIA INSTITUTE OF TECHNOLOGY • ATLANTA, GEORGIA 30332

6 August 1976

Massachusetts Institute of Technology
Lincoln Laboratory
Distribution Office
Lexington, Massachusetts 02173

ATTENTION: Dr. Joseph Katz

REFERENCE: Purchase Order No. CX-1069

SUBJECT: Project Status Report No. 2

Gentlemen:

A summary of the technical progress on the reference contract covering the period 1 July 1976 through 31 July 1976 is contained herein.

Technical Progress

Installation of the additional range gates and timing circuitry was completed on schedule. However, unexpected problems in interfacing the new circuits and a failure of the magnetron in transmitter No. 2 has caused a three-week delay in beginning the final radar checkout. Preliminary tests of the radar have been conducted and final checkout of the system will be accomplished on the Georgia Tech campus during the week of 9 August 1976. Operations at the field test site are expected to begin on 16 August 1976 and will extend over a period of two to three weeks.

Georgia Tech has not received a commitment from either the National Guard or the Marine Corps to furnish a target vehicle for the measurements; however, a concurrent program through ECOM has requirements for short pulse signatures of military vehicles, and the possibility of a combined field operation is being considered. If these arrangements are not possible, it is requested that the MIT Lincoln Laboratory assist Georgia Tech in procuring a target vehicle.

Analysis of the winter foliage penetration data was begun during the current reporting period. Work on this task will continue through August 1976.

Future Efforts

Evaluation of the radar will continue through 13 August 1976. At that time the radar van will be secured for transport to the field site.

Massachusetts Institute of Technology
Project Status Report No. 2
Page 2
6 August 1976

Data collection at the field site is expected to continue through the next reporting period and will be completed by 6 September. Work on a computer program to convert the data taken in the field to a calibrated digital format will begin during the next reporting period.


A revised Milestone Chart reflecting the effect of a three-week delay caused by problems encountered in interfacing the new instrumentation with the radar is attached. This delay is not expected to cause a delay in the completion of the overall program objectives.

Respectfully submitted,

E. E. Martin
Research Engineer
Project Director

EEM/nlj

Approved:

J. L.  Neaves, chief, Radar Technology Division

[illegible]



ENGINEERING EXPERIMENT STATION

GEORGIA INSTITUTE OF TECHNOLOGY • ATLANTA, GEORGIA 30332

22 September 1976

Massachusetts Institute of Technology
Lincoln Laboratory
Lexington, Massachusetts 02173

ATTENTION: C. W. Cahalane

REFERENCE: Purchase Order No. CX1069

SUBJECT: Report of Project Expenditures Exceeding 75%
of Total Contract Value.

Gentlemen:

Expenditures on the referenced purchase order will exceed 75% of the total contract within the next 30 days. An estimate of the cost to complete the required work is given below:

Estimated total cost for September	\$8,836.
Estimated total cost for October	\$6,359.

It is expected that delivery of the Final Report will be delayed until approximately 30 October 1976; however, this time extension will not effect the total contract cost.

Respectively submitted,

E. E. Martin
Project Director

Approved:

J. L. Leaves, Chief, Radar Technology Division



ENGINEERING EXPERIMENT STATION

GEORGIA INSTITUTE OF TECHNOLOGY • ATLANTA, GEORGIA 30332

22 September 1976

Massachusetts Institute of Technology
Lincoln Laboratory
Distribution Office
Lexington, Massachusetts 02173

ATTENTION: Dr. Robert Stovall

REFERENCE: Purchase Order No. CS-1069

SUBJECT: Project Status Report No. 3

Gentlemen:

A summary of the technical progress on the reference contract covering the period 1 August 1976 through 31 August 1976 is contained herein.

Technical Progress

Dr. S. N. Cole has been assigned to this program for the purpose of developing a computer program to create calibrated digital tapes from data collected during the field operations. Dr. Cole has an extensive background in mathematical modeling and computer simulations and is well qualified to conduct this task. Approximately 50% of the computer program development has been completed. A site near Pine Mountain, Ga. was selected as the location for the field measurements. A depression angle of 5.5 degrees at a range of approximately 0.75 miles is available at this location. Arrangements were made through ECOM to have Fort Benning supply a Jeep, a 2-1/2 ton truck and a 105 mm howitzer for use on a concurrent program being conducted by Ga. Tech. These vehicles are available on a non interference basis for use in the correlation measurements.

Final checkout of the measurements radar was completed and the van was driven to the Pine Mountain site on 16 August 1976. Verification of the system operation was completed on 17 August and data collection began on 18 August. The army vehicles arrived at the measurements site on 23 August and are expected to be available through the first week of September. Approximately 200 data samples have been collected on the jeep and 100 data samples have been collected on tree foliage. A 60 MHz frequency discriminator was installed on the radar to enable a more exact measurement of frequency differences between the two local oscillators. The addition of the frequency discriminator will allow a reduction in the uncertainty of the frequency difference between the two transmitters.

Analysis of the winter foliage penetration data continued through the current reporting period.

Future Efforts

Data collection at the field site will continue through 10 September 1976. At that time the radar will be returned to the Ga. Tech campus and the data reduction and analysis task will begin. It is expected that data reduction and analysis will require approximately three weeks.

Respectively submitted,

E. E. Martin
Project Director

Approved

J. L. Eaves, Chief, Radar Technology Division

TASK WEEK	JUNE			JULY				AUGUST					SEPTEMBER			
	14	21	28	5	12	19	26	2	9	16	23	30	6	13	20	27
<u>TASK I</u>																
Radar Modifications																
Radar Test																
Data Collection																
Data Analysis																
Computer Program																
Data Conversion																
<u>TASK II</u>																
Data Analysis																
Preparation of Draft Report																
Final Report																



ENGINEERING EXPERIMENT STATION

GEORGIA INSTITUTE OF TECHNOLOGY • ATLANTA, GEORGIA 30332

22 September 1976

Massachusetts Institute of Technology
Lincoln Laboratory
Lexington, Massachusetts 02173

ATTENTION: C. W. Cahalane

REFERENCE: Purchase Order No. CX1069

SUBJECT: Monthly Fiscal Status Report No. 3

Gentlemen:

A summary of the fiscal status of the referenced contract purchase order covering the period 1 August 1976 through 31 August 1976 is contained herein.

	<u>Month</u>	<u>Total to Date</u>
Engineering man-hours expended	418	833
Total man-hours expended	464	891
Funds Expended	\$8,080.	\$14,804.
Estimated fiscal material commitment	\$ 595.	\$ 657.

It is anticipated that work under this contract will be completed within the contract commitment.

Respectfully submitted,

E. E. Martin
Project Director

Approved:

J. L. Eaves, Chief, Radar Technology Division



ENGINEERING EXPERIMENT STATION

GEORGIA INSTITUTE OF TECHNOLOGY • ATLANTA, GEORGIA 30332

18 October 1976

Massachusetts Institute of Technology
Lincoln Laboratory
Distribution Office
Lexington, Massachusetts 02173

ATTENTION: Dr. Robert Stovall

REFERENCE: Purchase Order No. CX-1069

SUBJECT: Project Status Report No. 4

Gentlemen:

A summary of the technical progress on the reference contract covering the period 1 September 1976 through 30 September 1976 is contained herein.

Technical Progress

Data collection activities at Pine Mountain, Georgia, were concluded on 17 September 1976. Support vehicles supplied by the Army Infantry Center at Ft. Benning were withdrawn at that time. The vehicles were returned before all of the desired data could be collected; however, a significant portion of the data (approximately 1000 runs) were recorded on magnetic tape during the five week field operation. A summary of the recorded data is given below:

Table III Data

<u>Target</u>	<u>Polarization</u>	<u>No. Log Data Runs</u>	<u>No. Lin Data Runs</u>
Jeep	V	52	50
	H	52	50
2 $\frac{1}{2}$ Ton Truck	V	70	85
	H	70	65
	Circular	100	55
Field	V	80	85
	H	80	40
	Circular	100	45

Massachusetts Institute of Technology
Purchase Order No. CX-1069
Page 2
18 October 1976

Table IV Data

<u>Target</u>	<u>Polarization</u>	<u>No. Log Data Runs</u>	<u>No. Lin Data Runs</u>
True Foliage	V	22	27
	H	22	27
	Circular		15
*Howitzer	V	9	9
	H	9	9

*Linear data was substituted for phase data

Analysis of the data was begun on 20 September 1976. However, a malfunction developed in the correlator used to compute the correlation function and the unit was returned to the manufacturer for repair. The manufacturer has promised to look at the correlator immediately upon receipt, although a two week repair time is expected. Reduction and analysis of the correlation data will require approximately one week after the correlator is returned. A computer program for creating a digital data tape is approximately 95 per cent complete, with only a small verification task remaining. Final verification of the program will be accomplished on data recorded during the field operations.

The data reduction task for the winter foliage penetration measurements is approximately 80 per cent complete. Efforts are presently underway to analyze the data for comparison to the previous summer measurements.

Future Efforts

Preparation of the draft report and calibrated data tape will begin early in the next reporting period. However, completion of the report will be delayed until the correlator is returned from the manufacturer.

Respectfully submitted,

E. E. Martin
Project Director

Approved:

J. L. Eaves, Chief, Radar Technology Division



ENGINEERING EXPERIMENT STATION
GEORGIA INSTITUTE OF TECHNOLOGY • ATLANTA, GEORGIA 30332

17 October 1976

Massachusetts Institute of Technology
Lincoln Laboratory
Lexington, Massachusetts 02173

ATTENTION: C. W. Cahalane

REFERENCE: Purchase Order No. CX1069

SUBJECT: Monthly Fiscal Status Report No. 4

Gentlemen:

A summary of the fiscal status of the referenced contract purchase order covering the period 1 September 1976 through 30 September 1976 is contained herein.


	<u>Month</u>	<u>Total to Date</u>
Engineering man-hours expended	\$ 324.	\$ 1,157.
Total man-hours expended	384.	1,275.
Funds expended	6,781.	21,051.
Estimated fiscal material commitment	388.26	795.

It is anticipated that work under this contract will be completed within the contract funding.

Respectfully submitted,

E. E. Martin
Project Director

Approved:

J. L.  Hayes, Chief, Radar Technology Division



ENGINEERING EXPERIMENT STATION

GEORGIA INSTITUTE OF TECHNOLOGY • ATLANTA, GEORGIA 30332

10 January 1977

Massachusetts Institute of Technology
Lincoln Laboratory
Distribution Office
Lexington, Massachusetts 02173

ATTENTION: Dr. Robert Stovall

REFERENCE: Purchase Order No. CX-1069

SUBJECT: Project Status Report No. 5

Gentlemen:

A summary of the technical progress on the reference contract covering the period 1 October 1976 through 30 November 1976 is contained herein.

Technical Progress

The data reduction and analysis task for both the correlation measurements and the winter foliage penetration measurements have been completed. Preparation of the final report is nearing completion and will be delivered in early January. Several circuit failures occurred during attempts to digitize the analog data. These failures have caused a delay in verifying the computer program for generating the calibrated data tape; however, the A/D converter is presently operational, and it is anticipated that conversion of the data to a digital format will be accomplished during the first week of January. An additional period of two weeks is expected for program verification and generation of the calibrated data tape. The calibrated data tape and documentation of the tape format are expected to be delivered during the last week of January.

Respectfully submitted,

E. E. Martin
Project Director

Approved:

J. L. Eaves
Chief, Radar Technology Division



ENGINEERING EXPERIMENT STATION

GEORGIA INSTITUTE OF TECHNOLOGY • ATLANTA, GEORGIA 30332

20 January 1977

Massachusetts Institute of Technology
Lincoln Laboratory
Lexington, Massachusetts 02173

ATTENTION: C. W. Cahalane

REFERENCE: Purchase Order No. CX1069

SUBJECT: Monthly Fiscal Status Report No. 5

Gentlemen:

A summary of the fiscal status of the referenced contract purchase order covering the period 1 October 1976 through 30 November 1976 is contained herein.

	<u>Oct/Nov</u>	<u>Total to Date</u>
Engineering man-hours expended	470	1,627
Total man-hours expended	54	1,329
Funds Expended	\$9,578	\$30,629
Estimated fiscal material commitment	\$ 400	\$ 985

Respectfully submitted,

E. E. Martin
Project Director

Approved:

J. L. Eaves
Chief, Radar Technology Division

A-1858



ENGINEERING EXPERIMENT STATION

GEORGIA INSTITUTE OF TECHNOLOGY • ATLANTA, GEORGIA 30332

15 February 1977

Massachusetts Institute of Technology
Lincoln Laboratory
Distribution Office
Lexington, Massachusetts 02173

ATTENTION: Dr. Robert Stovall

REFERENCE: Purchase Order No. CX-1069

SUBJECT: Project Status Report No. 6

Gentlemen:

A summary of the technical progress on the reference contract covering the period 1 December 1976 through 31 January 1977 is contained herein.

Technical Progress

Three copies of the Approval Draft of the Final Technical Report, covering work accomplished on this program, were submitted. A computer program for digitizing, calibrating, and formatting the analog data recorded during the Pine Mountain field operations has been completed. The format of the digitized data contained on the final data tape is described in Attachment I, "Format of Radar Recordings on Magnetic Tape". Parameters used during the data collection are shown in Attachment II. Each data run included in the digital data tape consists of two data runs recorded in the field. The first half of the digital data corresponds to the first polarization shown in Attachment II. The last half of the run corresponds to the second polarization indicated.

A table of contents of the runs on the data tape is included as Attachment III. Abbreviations used in describing the data are shown below.

<u>Computer Tape Identification</u>	<u>Signal</u>
PARA., P	Parallel polarized signal
CROSS, C	Cross polarized signal
SIN	Sine of the angle between the parallel and cross polarized signals
COS	Cosine of the angle between the parallel and cross polarized signals

Massachusetts Institute of Technology
Project Status Report No. 6
Page 2
15 February 1977

<u>Computer Tape Identification</u>	<u>Signal</u>
F1	Fixed frequency
F2	Variable frequency
R1	Range cell 1
R2	Range cell 2

The computer listing of the Table of Contents identifies data by run number. These run numbers should be matched with run numbers in Attachment II for determination of the corresponding radar parameters.

All tasks required by the Statement of Work has been completed, with the exception of publication of 25 copies of the final report. This remaining task will be completed within 30 days after receipt of the approved draft.

Respectfully submitted,

Attachments: 3

E. E. Martin
Project Director

Approved:

J. L. Eaves, Chief
Radar Technology Division

GEORGIA INSTITUTE OF TECHNOLOGY
Engineering Experiment Station
Atlanta, Georgia 30332

FINAL REPORT

Project A-1858

PART I

CORRELATION PROPERTIES OF RADAR TARGETS AT Ku-BAND

by

E. E. Martin

Prepared for:

Lincoln Laboratory
Massachusetts Institute of Technology
Lexington, Massachusetts 02173
Under
Contract No. CX-1069

ABSTRACT

Two measurements programs were conducted by the Engineering Experiment Station at Georgia Tech. The first program concerned the correlation properties of radar targets when illuminated by a frequency diversity Ku-band radar. Data were collected on a 2 1/2 ton truck, medium dense tree clutter and on a grass covered field. Auto-correlation functions were computed for each pair of frequencies and correlation coefficients were calculated. These data are presented as plots of the correlation coefficient vs. frequency separation. The normalized autocorrelation coefficients for grass and tree clutter targets indicate that a $\sin x/x$ function is a good approximation to the expected decorrelation as a function of frequency separation. The magnitude of the decorrelation and the frequency separation required to produce decorrelation of distributed targets such as the 2 1/2 ton truck appear to be related to the orientation of the major scattering centers within the target complex.

The second measurements program extends the previous data collected for summer foliage penetration to include winter one-way penetration of deciduous trees. These winter penetration data were collected at X-band and Ku-band at a depression angle of approximately 29 degrees. Attenuation coefficients based on a per layer foliage definition and a total path definition were computed and compared to the data collected earlier. Except for defoliation of the tree branches, identical location, equipment, and conditions were maintained for these measurements as those for the earlier summer measurements.

TABLE OF CONTENTS

ABSTRACT	iii
PART I	1
1. INTRODUCTION	1
1.1 Background	1
1.2 Autocorrelation	2
2. DESCRIPTION OF MEASUREMENTS	5
2.1 Measurement Goals	5
2.2 Ku-Band Instrumentation Radar	5
2.3 Signal Processing Equipment	7
2.4 Field Site and Targets	7
2.4.1 Description of Field Site	7
2.4.2 Description of Targets	11
2.5 Measurement Procedures	11
2.5.1 Frequency Measurement Accuracy	15
2.5.2 Calibration Procedures	15
2.5.3 Data Collection Procedures	16
3. CORRELATION DATA ANALYSIS	19
3.1 Analysis Procedure	19
3.2 Results of Correlation Analysis	19
3.2.1 M35A2-2 1/2 Ton Cargo Truck	19
3.2.2 Clutter Targets	21
4. CONCLUSIONS AND RECOMMENDATIONS	29
PART II	31
5. INTRODUCTION	33
A. Background	33
B. Description of Field Measurements	34
1. Description of Summer Measurements	34
2. Description of Winter Measurements	55
6. DATA RESULTS	59
A. Data Analysis Techniques	59
1. Data-Reduction Facility	59
2. Data Analysis Procedure	59

B.	Summary of Results	60
1.	Interpretation of the Data	60
2.	Penetration Data Summary	63
7.	CONCLUSIONS AND RECOMMENDATIONS	77
REFERENCES	81

LIST OF FIGURES

PART I

Figure 1.	Block Diagram of Ku-Band Instrumentation Radar . . .	6
Figure 2.	Oscilloscope Trace Showing the Two Transmitter Pulses	8
Figure 3.	Block Diagram of Signal Conditioning and Recording Section of Ku-Band Radar	10
Figure 4.	Photograph Taken from Radar Location Showing Target Site	12
Figure 5.	Photograph Taken from Target Location Showing Radar Site	12
Figure 6.	Measurement Site Showing Location of 2 1/2 Ton Truck and Clutter Cell	13
Figure 7.	M35A2 2 1/2 Ton Cargo Truck at Measurements Site . .	14
Figure 8.	Autocorrelation Coefficient vs. $\tau\Delta f$ for M35A2 2 1/2 Ton Cargo Truck at an Azimuth Angle of 75° on a Depression Angle of 5.5°	20
Figure 9.	Autocorrelation Coefficient vs. $\tau\Delta f$ for M35A2 2 1/2 ton Cargo Truck at an Azimuth Angle of 45° on a Depression Angle of 5.5°	22
Figure 10.	Autocorrelation Coefficient vs. $\tau\Delta f$ for M35A2 2 1/2 ton Cargo Truck at an Azimuth Angle of 45° and a Depression Angle of 5.5°	23
Figure 11.	Autocorrelation Coefficient vs. $\tau\Delta f$ for Field Covered with 3-6 Inch Tall Grass	24
Figure 12.	Normalized Autocorrelation Coefficient vs. $\tau\Delta f$ for Field Covered with 3 to 6 Inch High Grass . . .	26
Figure 13.	Autocorrelation Coefficient vs. $\tau\Delta f$ for Deciduous Tree Foliage. Depression Angle 5.5°	27
Figure 14.	Normalized Autocorrelation Coefficient vs. $\tau\Delta f$ for Medium Dense Deciduous Tree Foliage	28

LIST OF FIGURES (Continued)

PART II

- Figure 15. Aerial View of Test Site 1 Showing Radar Van and
and Surrounding Foliage Areas 35
- Figure 16. Photograph of Typical Deciduous Tree Area Near
Test Site 1 35
- Figure 17. Photograph of Young Pine Grove at Test Site 2 . . . 36
- Figure 18. Photograph of Oak Tree at Test Site 3 36
- Figure 19. Geometry of One-Way Large Depression Angle
Experiment 38
- Figure 20. Photograph of Test Radar Van Located At Test
Site 1 39
- Figure 21. Simplified Block Diagram of Equipment Configuration
of Typical Instrumentation Radar. 45
- Figure 22. Close Up View of Radar Antennas 46
- Figure 23. Block Diagram of Equipment Configuration Used in
One-Way Measurements 49
- Figure 24. Remote Transmitters and Transmitting Horns Used
in One-Way Experiments 50
- Figure 25. Illustration of the Effect of Ground Reflections on
the Field Pattern of the Radar 53
- Figure 26. View of the Transmitter Site from the Receiving
Antennas Looking Through the Defoliated Oak Tree. . 56
- Figure 27. View of the Radar Vans and Receiving Antennas
Used for the Winter Measurements 56
- Figure 28. Comparison of the Summer/Winter Values Measured
for the Foliage Attenuation Coefficient of a
Water Oak Tree as a Function of Foliage Depth,
9.4 GHz, 29° depression angle 68
- Figure 29. Comparison of the Summer/Winter Values Measured
for the Foliage Attenuation Coefficient of a
Water Oak Tree as a Function of Foliage Depth,
16.2 GHz, 29° depression angle 69

LIST OF FIGURES (Continued)

PART II

- Figure 30. Summary of Attenuation Coefficient Results for
Low-Angle/High Angle, Summer/Winter Measurements
as a Function of Frequency 70
- Figure 31. Probability Distributions of the Relative Power
Received through a Tree Canopy for Winter/Summer
Foliage Conditions and Foliage Depths of 3.9 m
and 6.0 m, 9.4 GHz 71
- Figure 32. Probability Distributions of the Relative Power
Received Through a Tree Canopy for Winter/Summer
Foliage Conditions and Foliage Depths of 3.9 m
and 6.0 m, 16.4 GHz 72

LIST OF TABLES

Table 1.	GT-2 System Parameters and Features	9
Table 2.	Data Collection Formats	17
Table 3.	Parameters of Georgia Tech GT-1 Experimental Radar	40
Table 4.	Parameters of Georgia Tech GT-J Experimental Radar	41
Table 5.	Parameters of Georgia Tech GT-K Experimental Radar	42
Table 6.	Parameters of Georgia Tech GT-M Experimental Radar	43
Table 7.	Parameters for Remote Transmitters	47
Table 8.	Summary of One-Way Attenuation Measurements for Sites 1 and 2 (Summer)	62
Table 9.	Summary of Two-Way Attenuation Measurements (Summer)	63
Table 10.	Large Depression Angle Measurements (Summer)	64
Table 11.	Large Depression Angle Measurements (Winter)	66
Table 12.	Seasonal Attenuation Coefficient Changes Over Specific Radar Beam Paths	67

1. INTRODUCTION

1.1 Background

The ability of radar to detect small targets at the earth's surface is limited by the relatively large signal return from ground clutter. Improvement in the target-to-clutter ratio by signal averaging is limited in part by the relatively short dwell time on target when compared to the time that clutter returns remain correlated. The time required for a clutter target to decorrelate due to natural causes is a function of the distribution of the individual scatterers, environmental influences, and the frequency of the illuminating signal. Pulse-to-pulse frequency agility provides a means of reducing decorrelation time to a value approaching the interpulse period of the radar.

Some frequency agile radars currently in use employ variable time constant storage devices (either direct view storage tubes or digital storage and integration followed by a television format display) for integration and display of the radar signals. Returns from vegetation clutter, viewed on such a display, appear to break up into a granular structure as compared to the continuous structure seen on normal displays. Further improvements may be realized in frequency agile radars if signal processing techniques are implemented which more completely exploit the differences in frequency sensitivity between clutter and targets.

Under contract to the Lincoln Laboratory at the Massachusetts Institute of Technology, the Engineering Experiment Station at Georgia Tech conducted a limited series of measurements at Ku-band to determine the effect of pulse-to-pulse frequency separation on the correlation properties of radar targets. The targets were a 2 1/2 ton Army truck,

a grass covered field on which the truck was located, and medium to heavy tree clutter. Correlation coefficients of the radar reflectivity from these targets are presented as a function of $\tau\Delta f$, where τ is the radar pulse length and Δf is the pulse-to-pulse change in frequency.

1.2 Autocorrelation

The autocorrelation function provides a means for measuring the time required to obtain independence between samples of a given function. If independence between samples can be achieved, the mean values can be more rapidly estimated. This is particularly important when the number of samples (limited by the radar scan rate) is small. It provides a means for measuring (or predicting) the correlation properties of a function. The amplitude of a detected radar signal may be represented as the sum of a dc component plus an ac component. The autocorrelation function for a wave form of this type may be expressed as [1]

$$\phi_{(\tau)} = C^2 + \lim_{T \rightarrow \infty} \frac{1}{2T} \int_{-T}^T g_1(t)g_1(t - \tau) dt, \quad (1)$$

where C is the dc component of the signal, $g_1(t)$ is the ac component, and τ is the time delay for which $\phi_{(\tau)}$ is evaluated. It is equally valid to express equation (1) in the summation form for sampled processes such as pulsed radar.

The parameter investigated in these measurements is the amount of decorrelation which may be expected as a function of frequency separation between radar pulses (as opposed to time lag). This was accomplished by alternately transmitting on two frequencies and computing the autocorrelation function of the sampled video signal. The ratio of the autocorrelation function evaluated at $\tau = T$ and $\tau = 0$ gives the correlation coefficient as a function of frequency separation, where $\frac{1}{T}$ is the radar prf. This quantity, [2]

$$\hat{R}(\Delta f) \equiv \hat{R}(\tau = T) = \frac{\phi(\tau = T)}{\phi(\tau = 0)} = \frac{\phi(\Delta f)}{\phi(\Delta f = 0)} \quad (2)$$

represents the amount of decorrelation due only to the frequency separation provided the pulse repetition interval T is much less than the time decorrelation interval for the signal in question. In (2) the mean squared value of the autocorrelation function is retained. If the mean squared value of the autocorrelation function is removed, the normalized autocovariance

$$\rho(\Delta f) = \frac{\phi(\Delta f) - C^2}{\phi(0) - C^2} \quad (3)$$

is obtained. Since the correlation processor used to complete the correlation functions could not compute the C^2 value for multiple data runs, equation (3) was not suited for evaluating $\rho(\Delta f)$ for hard targets, i.e. targets for which the time variance was essentially zero. Equations (2) and (3) are used as appropriate in the evaluation of the correlation coefficients.

The relationship between frequency separation and the autocorrelation function has been predicted for certain clutter models [3] and for distributed targets [4]. An early investigation by Goldstein concerned with frequency instability in transmitters assumed a model of uniformly dense scatterers with randomly distributed phases. With this clutter model, the correlation coefficient becomes small when the pulse-to-pulse frequency separation equals the reciprocal of the pulsewidth. An exact mathematical prediction for range limited targets containing many scattering centers would be an exceedingly difficult task; however, for two scatterers spaced a distance D apart, one may readily verify that complete cancellation (decorrelation) would occur at a frequency separation of

$$\Delta f = \frac{c}{4D \cos \theta} \quad (4)$$

where c is the velocity of propagation and θ is the angle between the radar line of sight and a line connecting the two scatterers. Equation (4) may be expected to yield a minimum frequency separation required for decorrelation of a target with range extent less than a resolution cell and D as the maximum distance between scattering centers.

For clutter targets, a band limited noise spectrum has been assumed (1, 4) and the autocorrelation coefficient as a function of frequency has the form:

$$\phi_{(\Delta f)} = \frac{\sin \pi \tau \Delta f}{\pi \tau \Delta f} \quad (5)$$

Where a square law detector precedes the correlation process, (5) has the form:

$$\phi_{(\Delta f)} = \left[\frac{\sin \pi \tau \Delta f}{\pi \tau \Delta f} \right]^2 \quad (6)$$

In equations (5) and (6), $\phi_{(\Delta f)}$ goes to zero at a value of $\tau \Delta f = 1$. For non-uniformly distributed targets, no simple relationship exists and the correlation properties will be governed by the effect of constructive and destructive interference between major scattering centers that results as the transmission frequency is varied pulse-to-pulse. Equation (4) may be used only to indicate the minimum frequency separation for which some degree of decorrelation may occur; however, the actual frequency separation and the degree of decorrelation are most readily determined by measurements.

2. DESCRIPTION OF MEASUREMENTS

2.1 Measurement Goals

The goals of this program have been to determine the effects of frequency agility on the correlation properties of the radar reflectivity of vehicle and clutter targets and to record samples of amplitude and phase data from these targets. The amplitude and phase data were converted into calibrated digital tapes for later analysis at the Lincoln Laboratory. Technical areas addressed in the program included investigations of (1) how much clutter targets decorrelate as a function of frequency separation when illuminated by a radar transmitting on two alternate frequencies, and (2) the extent to which the return from vehicle targets remains correlated under these same conditions.

2.2 Ku-Band Instrumentation Radar (GT-2)

A Georgia Tech-owned instrumentation radar was used to gather the required data. This radar is a dual polarized Ku-band system equipped with two variable frequency transmitters and local oscillators. The transmitters may be triggered separately, simultaneously, or alternately as required. A block diagram of the system is shown in Figure 1. As shown on the block diagram, test ports are available for continuously monitoring the transmitter output power, pulse shape, and frequency. In addition, a frequency meter is available to measure the frequency of the local oscillators, and a test port is provided for monitoring the local oscillator drive levels.

The test port was used in these measurements to monitor the local oscillator frequency. The test port output was connected to a calibrated 60 MHz frequency discriminator. The voltage out of the discriminator was

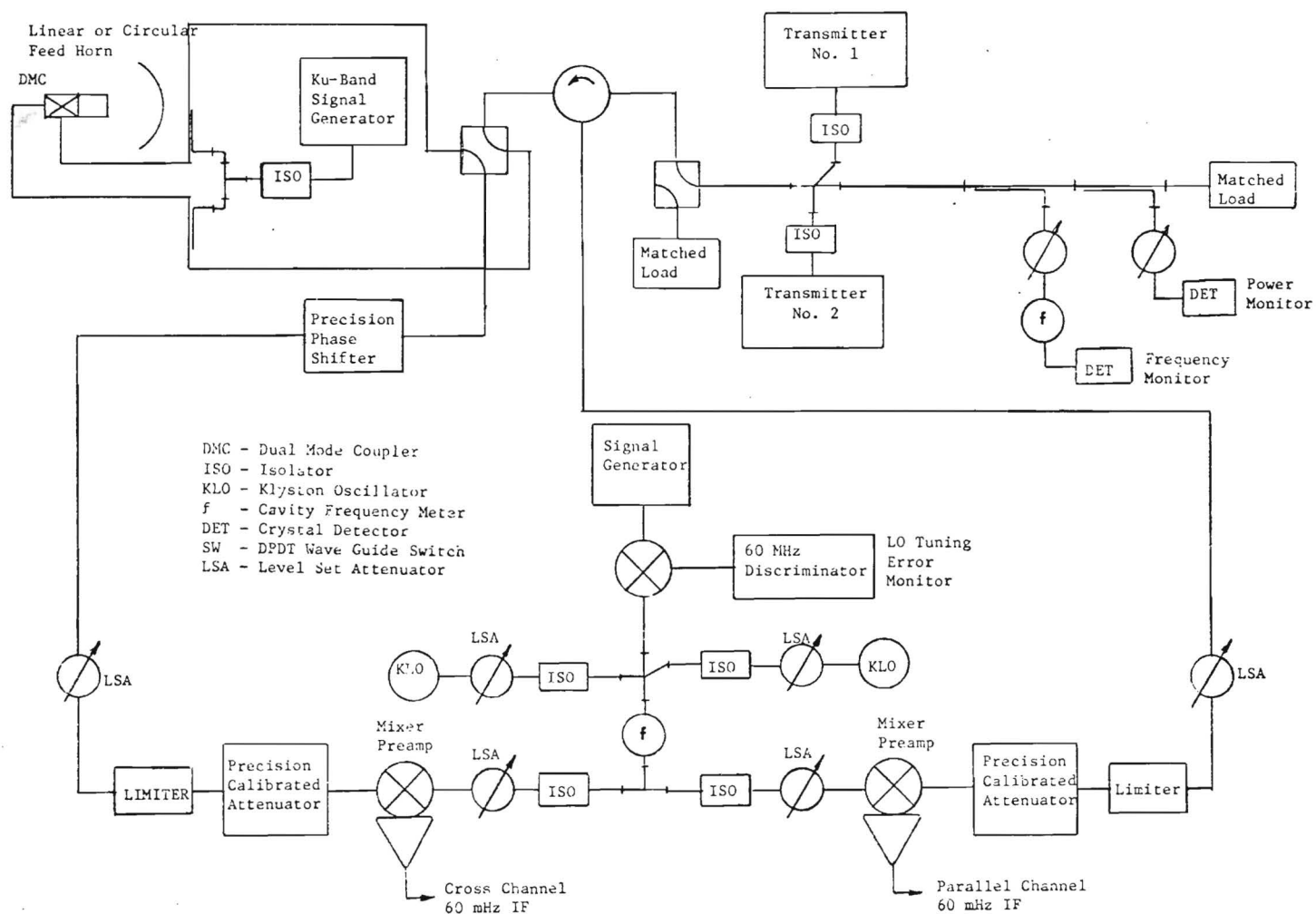


Figure 1. Block Diagram of Ku-Band Instrumentation Radar

then used to measure precisely the difference in frequency between the two local oscillators of GT-2. The GT-2 transmitters were tuned to a frequency 60 MHz above their respective local oscillators with an accuracy better than could be achieved by reading the frequency meter alone. The high voltage to the transmitters was adjusted to provide the nearest match between the two transmitted pulse shapes. A photograph of the pulse shapes for the two transmitters is shown in Figure 2.

The operating parameters of the GT-2 radar are listed in Table I. For these measurements the peak power delivered to the antenna, adjusted for the best match in pulse shape between the two transmitters, was 4.8 kW. The measurements were made at a pulse repetition rate of 1,024 Hz. Additional features of this radar include precision r.f. attenuators for calibration, level setting r.f. attenuators for matching the signal amplitudes in the parallel and cross channel receivers, and identical parallel and cross channel mixer/preamps.

2.3 Signal Processing Equipment

The data collected in these measurements required a receiver capable of both linear and logarithmic amplitude detection. In addition, the sine and cosine of the phase angle between the parallel and cross polarized radar returns was measured. Range gated boxcar samples of the signals were recorded on a 7-channel FM instrumentation tape recorder. A simplified block diagram of the i.f. section of the receiver and data sampling circuits is given in Figure 3. Since there were more signals to be recorded than available recorder channels, some of the data were interlaced (multiplexed) on two recorder channels.

A Nicolet Scientific Model UC202C Ubiquitous correlator was used to compute the correlation functions. This instrument is capable of computing autocorrelation, crosscorrelation, probability density functions, and cumulative distributions.

2.4 Field Site and Targets

2.4.1 Description of Field Site. The field site chosen for these measurements was located near the city of Pine Mountain, Georgia.

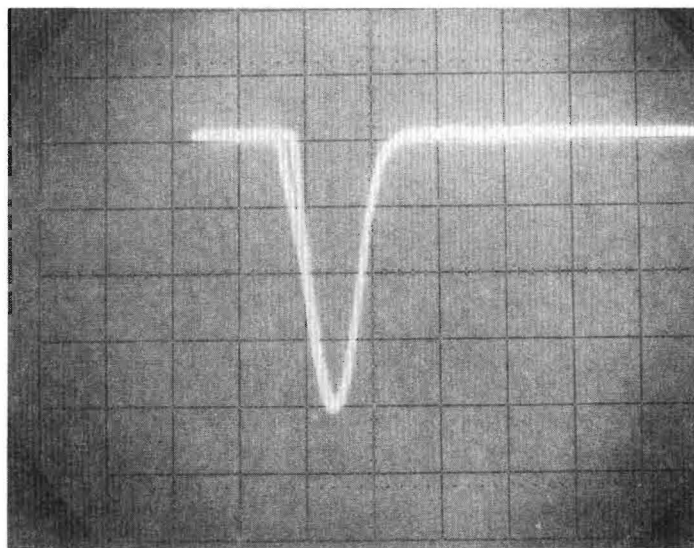


Figure 2. Oscilloscope Trace Showing the Two Transmitter Pulses.
Horizontal Scale, 100 ns/Division.

TABLE I
GT-2 SYSTEM PARAMETERS AND FEATURES

Frequency Diversity Dual Transmitters

RF frequency	15.9 - 16.4 GHz, each independently
Peak power	5 kW
Pulsewidth	80 nanoseconds
PRF	2 - 8 kHz
Firing modes at PRF	Either, alternately or simultaneously

Dual-Polarized Antenna

Type	Nonscanning 3-foot paraboloidal dish
Beamwidths	1.6°, parallel and orthogonal
Polarization modes:	
Transmit	Any fixed linear or either sense circular
Receive	Parallel and orthogonal components simultaneously regardless of transmit mode.
Azimuth adjustment	$\pm 180^\circ$, manual
Elevation adjustment	$- 20^\circ$ to $+ 90^\circ$, manual
Height of feed above ground	13.5 to 17.5 feet, manually adjustable in 0.5 feet increments

Receivers, Parallel and Orthogonal

Type	Integrated mixer - IF amplifier
Detection	Logarithmic Linear Phase Between P & C
Bandwidth	20 MHz 20 MHz
Dynamic Range	70 dB 25 dB
Sensitivity	-90 dBm -90 dBm

System Polarization Isolation 32 dB

Data Recording

Magnetic tape	7 channels, FM, 0 - 20 kHz
Oscillograph	6 channels, 0 - 5 kHz

System Power Internal power plant or external

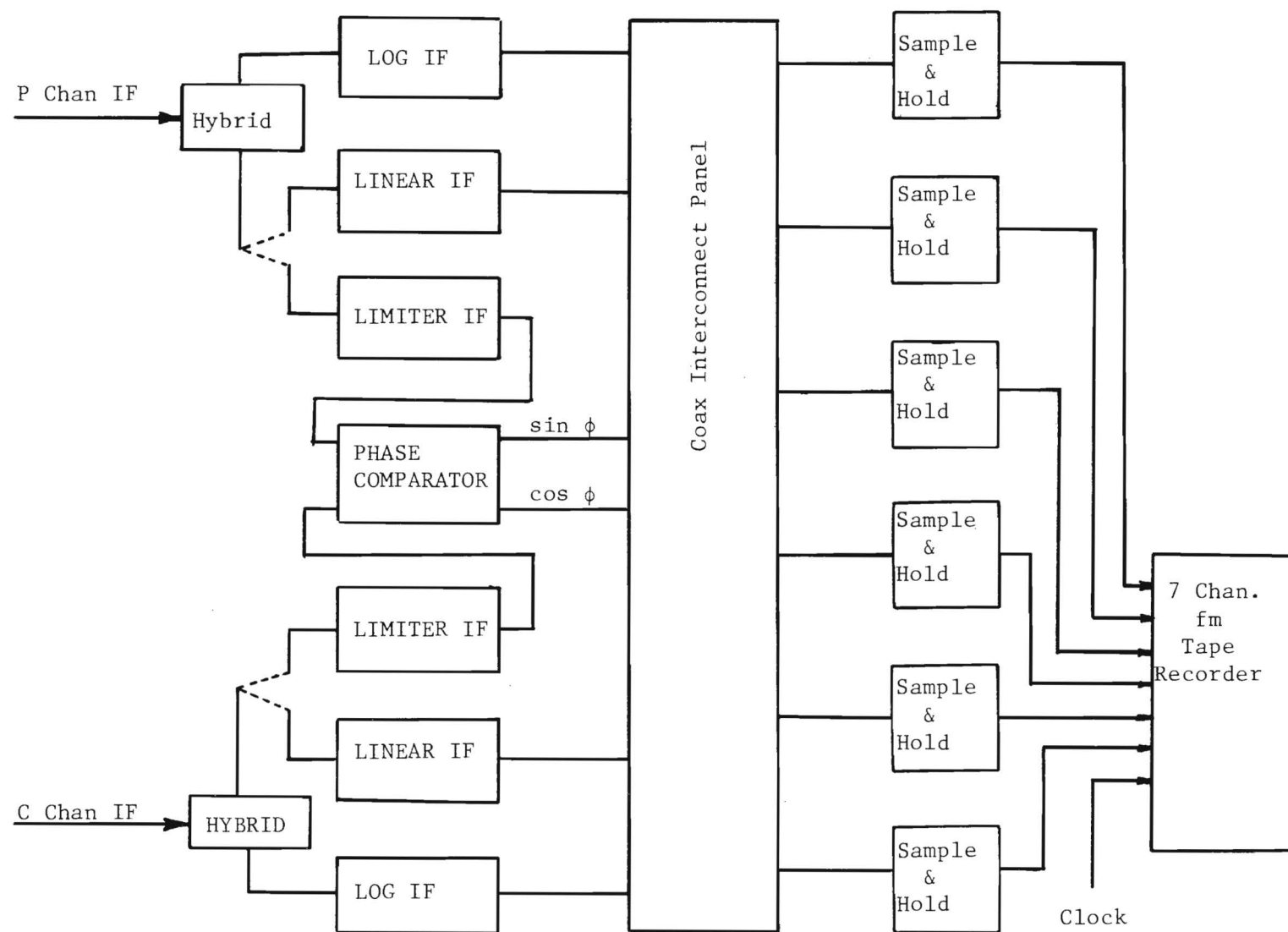


Figure 3. Block Diagram of Signal Conditioning and Recording Section of Ku-Band Radar

The site was chosen because of its proximity to both Atlanta and Ft. Benning and because it provided excellent opportunity to collect data on areas of trees and grass. The radar was located at a state-owned overlook known as Dowdell Knob. This location offered an excellent view from an elevation of approximately 125 meters above the surrounding forest and pasture lands. Figure 4 is a photograph taken from the radar location showing the target areas. The target vehicle was located in a privately owned pasture covered with grass which ranged in height from 7.6 to 15.2cm. A photograph of the radar site as seen from the target area is given in Figure 5.

The field in which the vehicles were located had a maximum dimension along the radial between the radar and target of approximately 100 meters. The target was located approximately 60 meters back from the fence line. A drawing showing the location of the target vehicle in relation to the road, fence, and tree line is shown in Figure 6. The radar was located at a slant range of 1.3 km from the vehicle. The geometry of this radar test range provided a depression angle of 5.5 degrees. For the 1.6 degree beam width of the antenna, the ground was illuminated 8.5 meters to either side of the vehicle center line.

2.4.2 Description of Targets. The primary vehicle target used in these measurements was an M35A2 2-1/2 Ton Cargo Truck. Figure 7 is a photograph of the truck showing the grass background. Data were collected simultaneously from the vehicle and from an area of the grass field approximately 21 meters in front of the vehicle. The area of trees from which data were collected is indicated in Figure 4. This area contained a variety of deciduous trees which ranged from 10 to 16 meters high. The depression angle and range from the radar to the tree location was 9.5 degrees and 890 meters respectively.

2.5 Measurement Procedures

The collection of radar data requires that careful attention be directed towards developing a set of procedures which will minimize errors introduced by the equipment as well as to the measurement techniques which

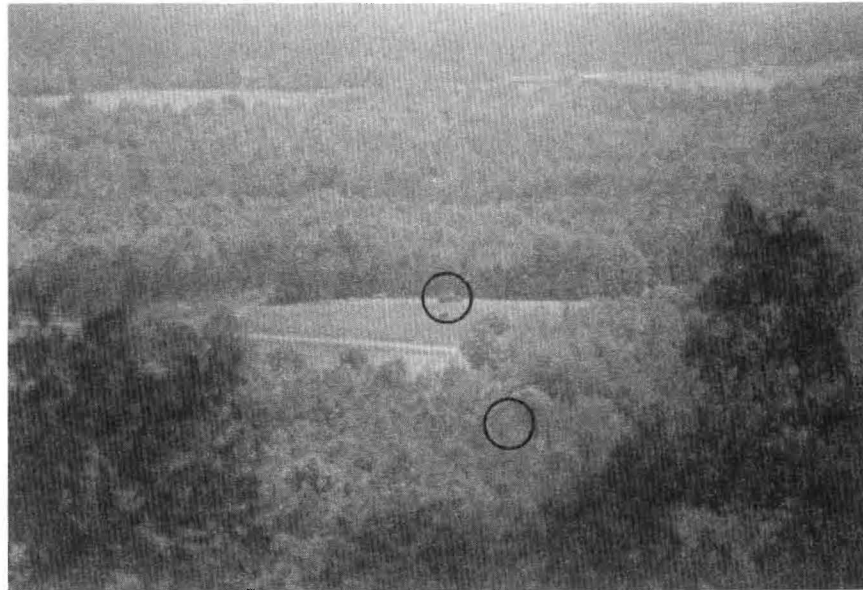


Figure 4. Photograph Taken from Radar Location Showing Target Site



Figure 5. Photograph Taken from Target Location Showing Radar Site

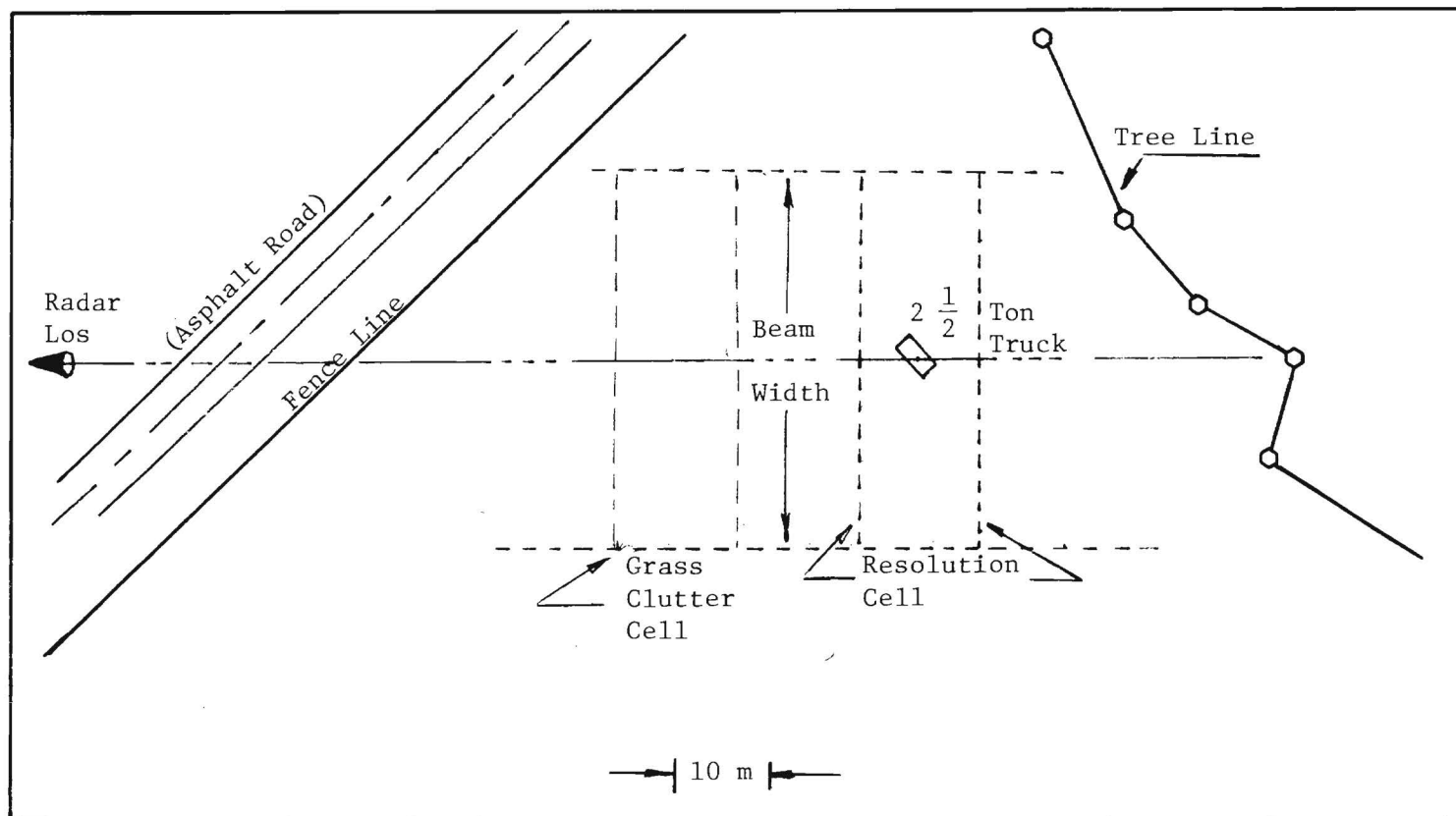


Figure 6. Measurement Site Showing Location of $2 \frac{1}{2}$ Ton Truck and Clutter Cell



Figure 7. M35A2 2 1/2 Ton Cargo Truck at Measurements Site.

are followed. This is necessary to insure that the data truly reflect the characteristics of the target. The first week of the field operation was devoted almost entirely to developing a set of procedures which allowed a high level of confidence in the measurements.

2.5.1 Frequency Measurement Accuracy. Perhaps the most critical operation in the collection of these data was the frequency change between each measurement. Therefore, particular emphasis was placed on establishing a method for measuring the frequency separation between the two transmitters and between the two local oscillators. Three methods of measuring the frequency separation were used. Two waveguide absorption frequency meters were used to establish absolute frequency of the transmitters and local oscillators. A frequency discriminator was installed at the local oscillator test port for continuous monitoring of the frequency difference between the two klystron local oscillators. The second frequency meter was used to calibrate the transmitter tuning dial in 10 MHz increments. The 10 MHz calibration marks were then linearly subdivided into 2 MHz increments. The calibrated transmitter dial proved to be the most accurate and repeatable method for tuning the transmitters to the desired frequency separation. Both incremental and absolute frequency measurements were made for each data run. Overall accuracy in the measurement of frequency separation of the local oscillators, using the calibrated discriminator, is approximately ± 0.5 MHz. Accuracy of the transmitter frequency separation is ± 1.3 MHz for small separations and degrades to the incremental accuracy of the frequency meter (± 2 MHz) for frequency shifts greater than 10 MHz.

2.5.2 Calibration Procedures. Calibration of the radar was established by injecting a known signal into the waveguide between the receiver and the antenna. The signal was simultaneously injected into both parallel and cross polarized receiver channels and compared to the signal received from a calibration target (triangular corner reflector) located near the target vehicle. The difference in signal level then establishes the peak value of the calibration in terms of the absolute radar cross-section. A receiver transfer characteristic was then

generated by stepping the precision wave guide attenuators in 10 dB steps from 0 to -50 dB. Each level is recorded on magnetic tape for use in calibrating data from the target. Range correction factors are applied to the calibration where needed to account for differences in range between the calibration standard and the target.

A phase calibration was achieved in a similar manner except that a precision r.f. phase shifter is used to generate the phase detector transfer characteristic.

2.5.3 Data Collection Procedures. Data were collected in three separate formats as indicated in Table II. A 7 channel FM tape recorder was used to record the signals listed under Formats I and II for later conversion to a calibrated digital data tape. The signals listed under Format III were recorded on FM tape except for the tree clutter targets. These data were reduced in the field using the model UC202C correlator.

Prior to calibration, the receivers were switched to the proper configuration for the selected data format. After suitable warmup and calibration the radar antenna was moved to the target position and a quick frequency sweep was made while observing the video return to determine a suitable reference frequency. This was necessary to prevent the selection of a "hole" in the frequency sensitivity characteristic of the target as a reference frequency. Once the reference frequency was selected both transmitters were tuned to this frequency, and range gates were positioned to the peak of the target's video signal. (Sample circuits in the radar are basically track and hold devices with 50 ns track windows). The sampled video was recorded on magnetic tape as full stretched boxcar signals representing either the amplitude of or the phase difference between the parallel and cross components of the received signals. Data were collected for horizontally, vertically, and right hand circularly polarized signals.

Each morning the 2 1/2 ton truck was positioned to a previously designated location and aspect angle (45 or 75 degrees). With both transmitters tuned to the same frequency, the sampled video was recorded

TABLE II
DATA COLLECTION FORMATS

FORMAT I			
Signal	Detection	Target	Frequency
1-P Channel	Logarithmic	2 1/2 Ton Truck	f_2
2-P Channel	Logarithmic	Field	f_2
3-P Channel	Logarithmic	2 1/2 Ton Truck	f_1
4-P Channel	Logarithmic	Field	f_1
5-C Channel	Logarithmic	2 1/2 Ton Truck	f_1/f_2
6-C Channel	Logarithmic	Field	f_1/f_2
7-Frequency ID	--	--	--

FORMAT II			
Signal	Detection	Target	Frequency
1-P Channel	Logarithmic	2 1/2 Ton Truck	f_2
1-C Channel	Logarithmic	2 1/2 Ton Truck	f_2
3-P Channel	Logarithmic	2 1/2 Ton Truck	f_1
4-C Channel	Logarithmic	2 1/2 Ton Truck	f_1
5-Sin ϕ	Phase-P/C	2 1/2 Ton Truck	f_1/f_2
6-Cos ϕ	Phase-P/C	2 1/2 Ton Truck	f_1/f_2
7-Frequency ID	--	--	--

FORMAT III			
Signal	Detection	Target	Frequency
1-P Channel	Logarithmic	2 1/2 Ton Truck	f_2
2-P Channel	Logarithmic	Field/Trees	f_2
3-P Channel	Logarithmic	2 1/2 Ton Truck	f_1
4-P Channel	Logarithmic	Field/Trees	f_1
5-P Channel	Linear	2 1/2 Ton Truck	f_1/f_2
6-P Channel	Linear	Grass Clutter	f_1/f_2
7-Frequency ID	--	--	--

for a period of one minute for correlation data or for 10 to 15 seconds for amplitude and phase data. In the linear polarization mode of transmission, the polarization was switched without stopping the tape recorder. Therefore, contiguous samples of data were obtained for vertical and horizontal polarizations. These runs were separated in time by approximately 1 second to allow time for the polarization switch to operate. After the data were recorded for the reference frequency, the frequency of one transmitter was changed in 2 MHz. increments until a sufficient number of data runs had been recorded to define the target's sensitivity to frequency change. The minimum frequency separation to cause decorrelation of the target was determined by applying Equation (4) to the maximum dimension of the truck. Normally frequency separations of at least twice the calculated value was used for the final Δf value.

3. CORRELATION DATA ANALYSIS

3.1 Analysis Procedure

The data collected in these experiments consisted of recorded samples of square law detected radar video. These data were analyzed at Georgia Tech at the conclusions of the operations using a Nicolet UC 202C correlator to compute the autocorrelation functions. Values of the autocorrelation functions at $\tau = 0$ and $\tau = T$, and the mean squared value were read from an oscilloscope display. Correlation functions were computed for each pair of frequencies over a 32 second sample of the input data. This time period represents the data acquired from 32,768 radar pulses. Values read from the oscilloscope were used to calculate the correlation coefficients using Equations (2) or (3) as appropriate.

3.2 Results of Correlation Analysis

3.2.1 M35A2-2 1/2 Ton Cargo Truck. Correlation coefficients were computed for the 2 1/2 ton truck using Equation (2). Typical correlation data for both horizontal and vertical polarizations and an aspect angle of 75 degrees are shown in Figure 8. For horizontal polarization it is seen that the signal remained highly correlated throughout the range of $\tau\Delta f$. However, when the target was illuminated by a vertically polarized transmitted signal a strong decorrelation was evident at a value of $\tau\Delta f = 1$ with a less significant decorrelation occurring at a value of $\tau\Delta f = 3$. No apparent periodicity in the correlation function was observed at this aspect angle over the range of measurements.

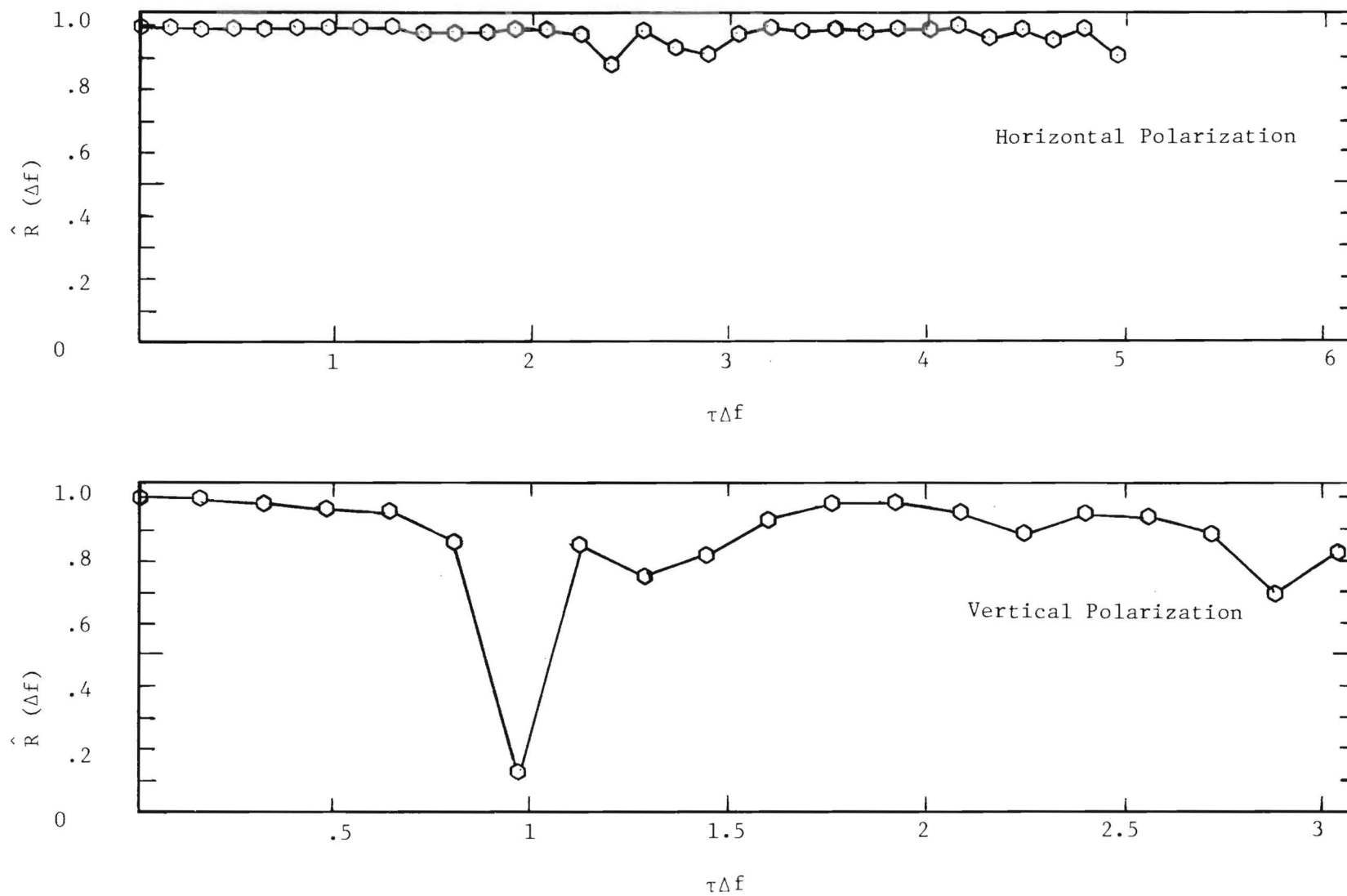


Figure 8. Autocorrelation Coefficient vs. $\tau\Delta f$ for M35A2 2 $\frac{1}{2}$ Ton Cargo Truck at an Azimuth Angle of 75 Degrees on a Depression Angle of 5.5 Degrees.

Another set of correlation data, taken at a target aspect angle of 45 degrees for horizontally and vertically polarized transmitted signals, is given in Figure 9. However, the data for vertically polarized transmission remains well correlated beyond a value of $\tau\Delta f = 6$ while data for the horizontally polarized signal had significant decorrelation for values of $\tau\Delta f$ near 2.5 and 4.5. Periodicity is not readily observable in these data; however, the data for circular polarization shown in Figure 10 indicates that a possible periodic decorrelation occurred. at $\tau\Delta f$ values of 0.8, 2.2, 4, and 5.1. The average frequency separation between these points is 18.6 MHz. Solving Equation (4) for the distance between scattering centers, corresponding to a Δf of 18.6 MHz, results in a value of 4.0 meters. When viewed at 45 degrees, the target vehicle has two apparent diplane like intersections formed by the drivers side door and the front of the truck bed, and the intersection of the tail gate and the left side of the truck bed. The scaled distance between these two points is 4.2 meters, which within the measurement tolerances, is in good agreement with the four meters required to cause decorrelation. Verification that the decorrelations are actually periodic and that they were caused by the assumed major scattering centers would require a more extensive investigation.

3.2.2 Clutter Targets. A typical set of correlation coefficients versus $\tau\Delta f$ for the grassy field is given in Figure 11. For these data the correlation coefficients were calculated without removing the mean squared value. The measurements were made simultaneously with the truck data, shown in Figures 9 and 10, by positioning a second range gate to a range cell located 21 meters in front of the vehicle. For both horizontal and vertical polarizations, the data show a high mean squared value relative to the peak of the correlation curve. However, for circular polarizations a lower mean squared value is shown along with a more rapid decorrelation. The low variance observed in the individual measurements for linear polarizations may be attributed to the relatively large contribution from the ground itself rather than from the grass. Normalized auto-covariance

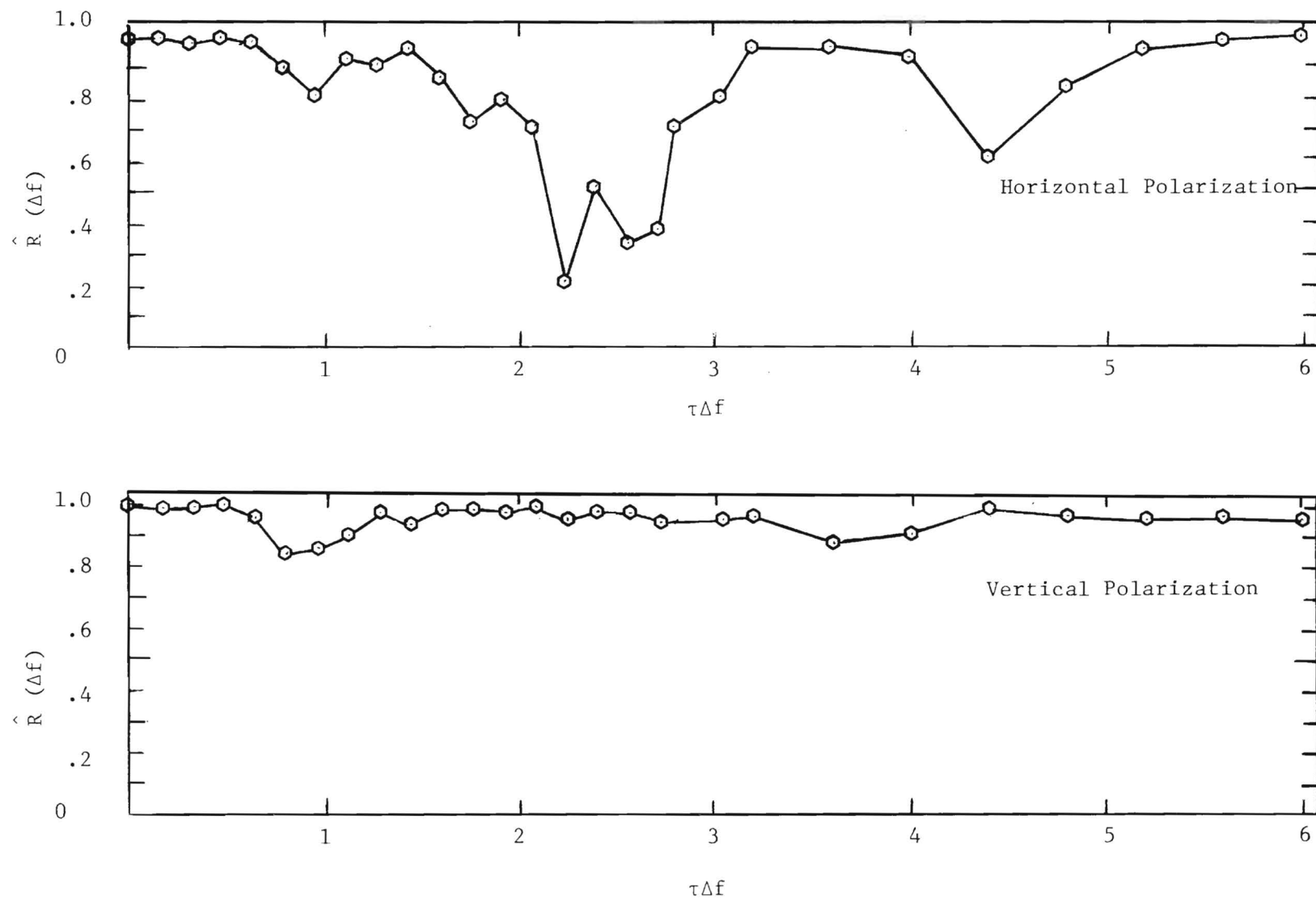


Figure 9. Autocorrelation Coefficient vs. $\tau\Delta f$ for M35A2 $2\frac{1}{2}$ ton Cargo Truck at an Azimuth Angle of 45 Degrees on a Depression Angle of 5.5 Degrees.

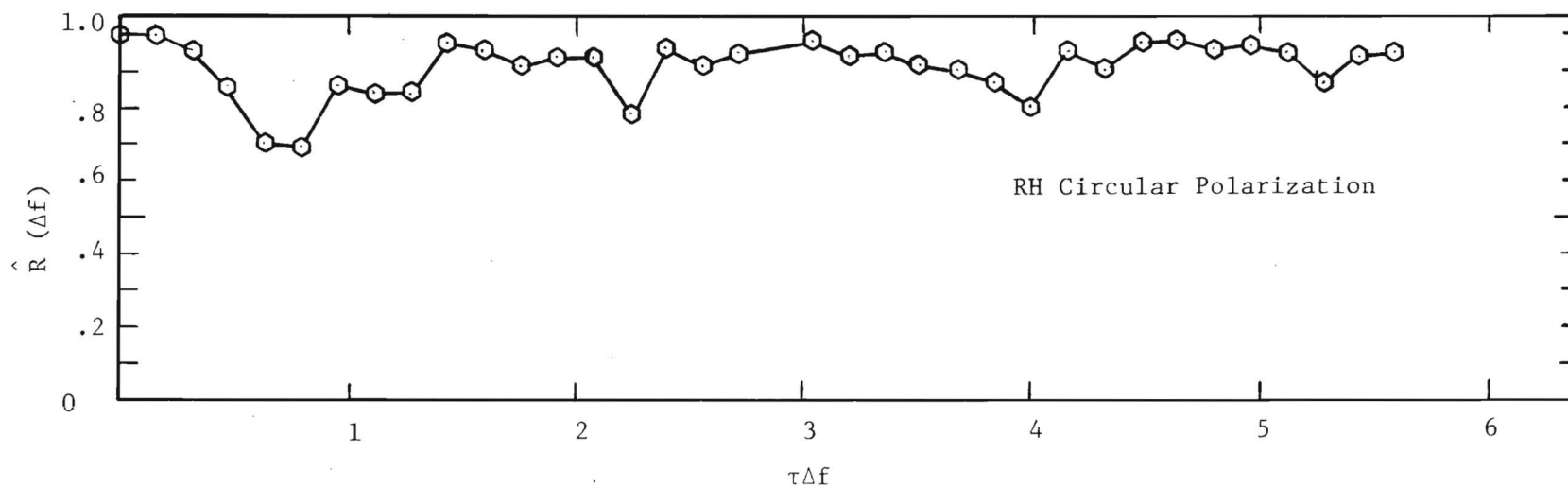


Figure 10. Autocorrelation Coefficient vs. $\tau\Delta f$ for M35A2 $2\frac{1}{2}$ Ton Cargo Truck at an Azimuth Angle of 45 Degrees and a Depression Angle of 5.5 degrees.

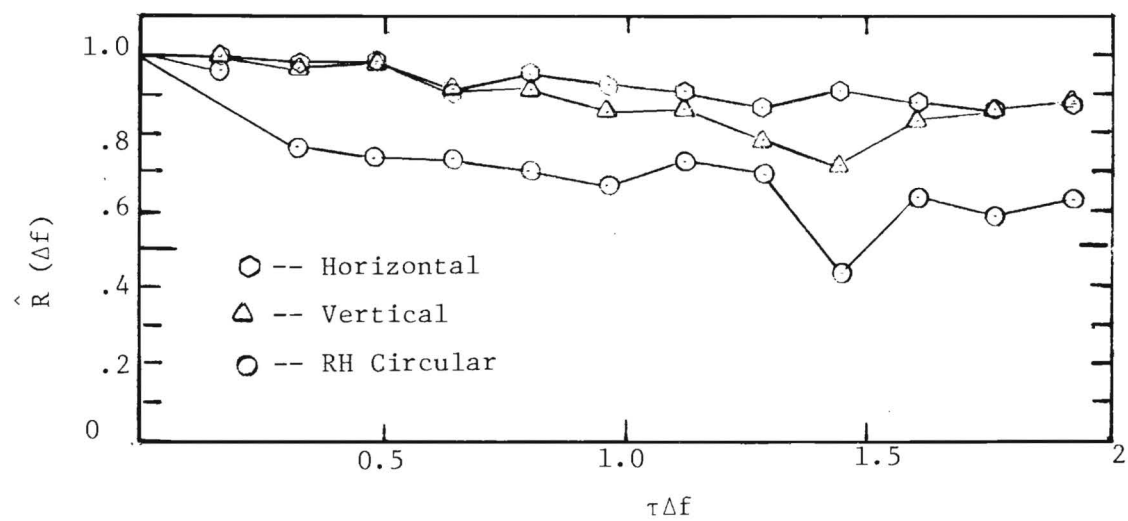


Figure 11. Autocorrelation Coefficient vs. $\tau\Delta f$ for Field Covered with 3-6 Inch Tall Grass. Depression Angle 5.5 Degrees

functions, calculated from equation (3), are shown in Figure 12 for these same data. $\sin x/x$ and $[\sin x/x]^2$ functions are plotted on the figure for comparison.

Auto-covariance functions computed from data for mixed deciduous trees, observed from a range of 0.89 km and at a depression angle of 9.5 degrees, are shown in Figures 13 and 14. Figure 13 shows the un-normalized correlation coefficient with the mean squared value falling below that of the grass. A closer approximation to the $\sin x/x$ curve is seen in the data plotted in Figure 14.

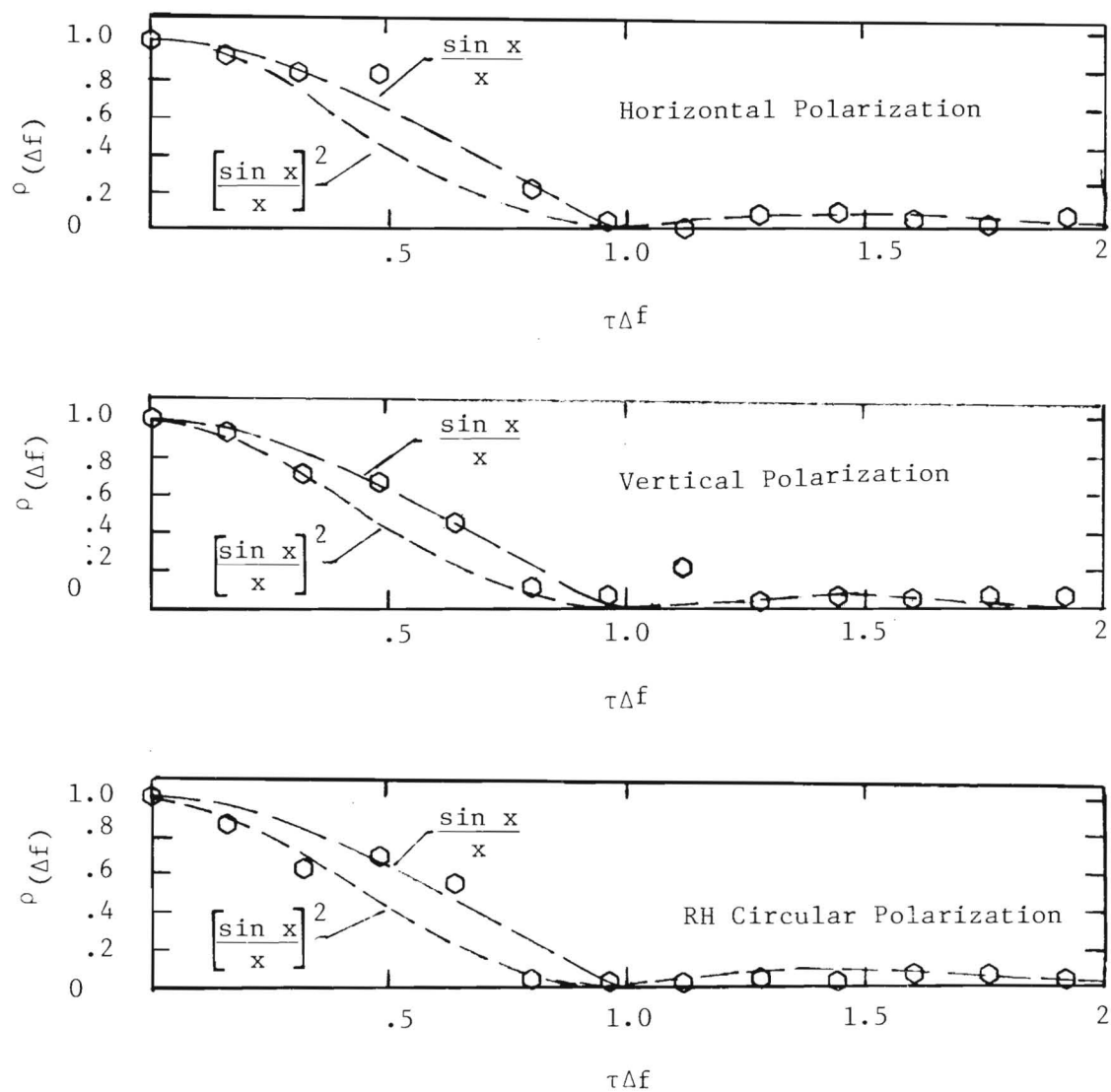


Figure 12. Normalized Autocorrelation Coefficient vs. $\tau\Delta f$ for Field Covered with 7 to 15 cm. High Grass

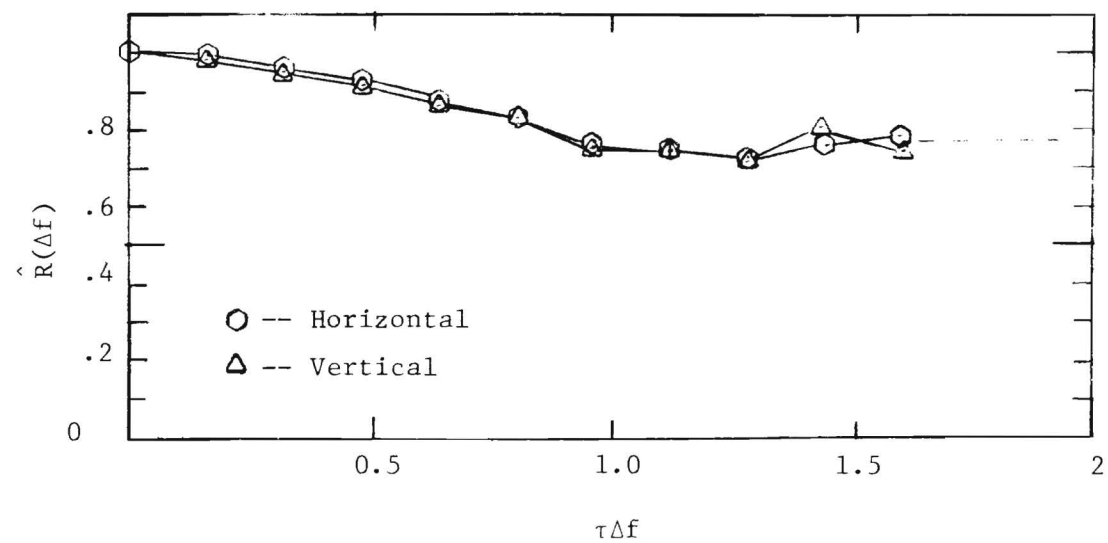


Figure 13. Autocorrelation Coefficient vs. $\tau\Delta f$ for Deciduous Tree Foliage. Depression Angle 5.5 Degrees

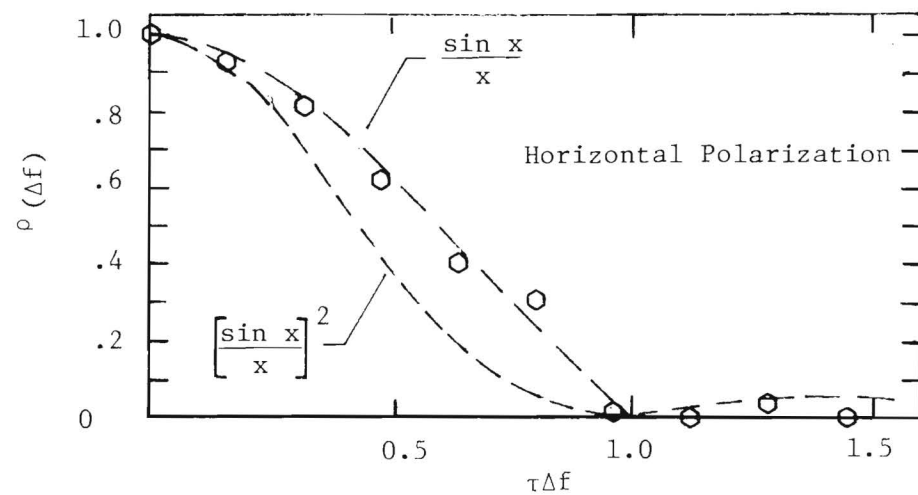
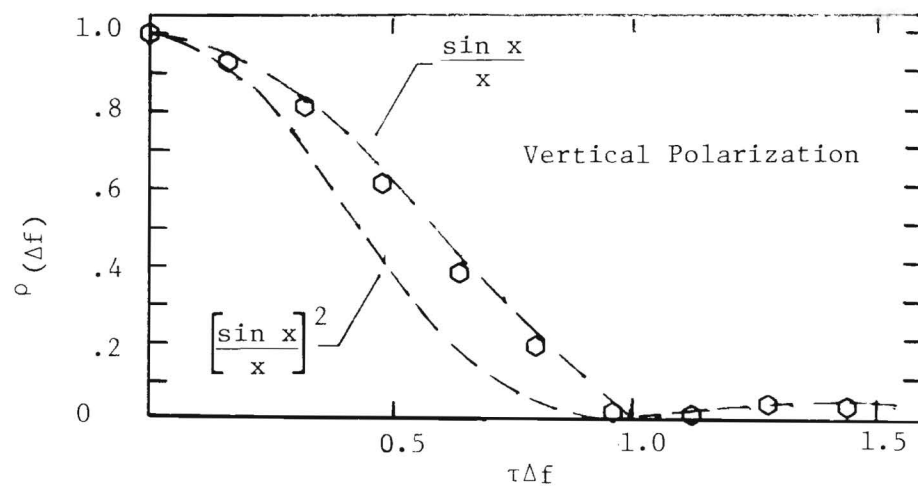


Figure 14. Normalized Autocorrelation Coefficient vs. $\tau\Delta f$ for Medium Dense Deciduous Tree Foliage. Depression Angle 9.1 Degrees.

4. CONCLUSIONS AND RECOMMENDATIONS

Results of the correlation analysis performed on the radar measurements tend to verify what might have been expected from a knowledge of the general behavior of complex targets. Both frequency sensitivity and aspect angle sensitivity exist and appear to be related to the constructive and destructive interference between dominant scattering centers of the target. From these measurements no trend was observed which would favor a given polarization, although at a given frequency there might exist a pronounced polarization dependence. The data shown in Figures 8, 9, and 10 indicate the desirability for having a large number of frequency steps if the full benefit from correlation processing is to be realized. Data from the tree clutter and grass clutter background indicate a minimum frequency separation between two successive radar pulses equal to the reciprocal of the pulsewidth is required for decorrelation. A practical lower limit on the number of frequency steps is related to the dwell time on the target so that each pulse would represent an independent sample. Decorrelation of tree and grass targets as a function of frequency spacing fall between a $\sin x/x$ and a $[\sin x/x]^2$ function.

The limited resources allocated to this program precluded a more extensive investigation of the correlation properties of the targets. There are additional areas which should be investigated to obtain a more complete description of target characteristics when illuminated with a frequency agile radar. It is suggested that consideration be given to a much broader measurements program to include the following areas for investigation.

a. Target Aspect Angle. In this program data were collected for correlation analysis only for two aspect angles. Because of the many lobed structure of the radar-cross-section vs. aspect angle of complex targets, further measurements should be conducted to better define the statistical variations in the correlation coefficients as a function of the aspect angle.

b. Dominant Scattering Centers. No attempt was made during the field operation to identify the dominant scattering centers which make up the composite radar return. It would be instructive to identify dominant scattering centers for those aspect angles and frequencies where either strong or periodic decorrelations occur.

c. Target Backgrounds. The target background for these measurements was a pasture covered with 7 to 15 cm tall grass. While the grass offered a reasonably good optical mask for the earth, sufficient energy from the radar penetrated the grass layer so that the earth itself strongly influenced the results of the measurements. Backgrounds of heavier grass cover, no grass cover, and rocky terrain should be considered in future measurement programs.

d. Multiple Frequency Illuminations. Two transmitters operating at frequencies separated by Δf were used to illuminate the target during these measurements. A better picture of the overall performance of frequency agile radars could be achieved with a radar capable of transmitting a sequence of pulses, each at a different frequency. Recorded signals from a fully frequency agile system are desirable for developing algorithms and computer simulations of signal processors.

e. Polarization. The data collected in these measurements indicate that there is a relationship among the polarization, frequency, and correlation coefficients. However, because of the limited scope of this program, insufficient data is available which would favor a given polarization. Additional measurements should be undertaken to determine if one polarization would offer an advantage over another. Since circular polarization appeared to produce a larger variance than linear polarization, comparative measurements should be made.

Frequency agility offers possibilities for implementing new signal processing algorithms which may significantly improve radar performance. Additional measurements should be made if the fullest benefits attainable with the latest technology in microwave and signal processing components are to be realized.

GEORGIA INSTITUTE OF TECHNOLOGY
Engineering Experiment Station
Atlanta, Georgia 30332

FINAL REPORT

Project A-1858

PART II

COMPARISON OF MICROWAVE WINTER/SUMMER FOLIAGE
PENETRATION MEASUREMENTS

by

N. C. Currie and T. P. Morton

5. INTRODUCTION

This report summarizes the results of a second phase of a measurement program to determine the characteristics of radar penetration of foliage at 10 GHz through 95 GHz which was conducted during the period August 1975 to October 1976. Emphasis in the report is placed on comparing the one-way attenuation properties of tree canopies for summer and winter foliage conditions at 10 GHz and 16 GHz, although two-way measurements for summer conditions only are also presented for 10 GHz, 16 GHz, 35 GHz, and 95 GHz.

A. Background

This program resulted from a need for information on the foliage penetration properties of radar signals in the region above 10 GHz which was identified by the Lincoln Laboratories, Massachusetts Institute of Technology. The work was intended to aid in the selection of the proper frequency band for a radar to be used in the mini-remotely-piloted-vehicle (mini-RPV) presently under development by the U.S. Army. The Engineering Experiment Station (EES) at Georgia Tech was selected to conduct the measurement program because of its expertise in the making of measurements in this frequency region as demonstrated by an on-going program for the Frankford Arsenal, U.S. Army, under Contract DAAA-25-73-C-0256. The initial phase of the measurement program was funded through Frankford Arsenal as an addition to Contract DAAA-25-73-C-0256, although this phase was performed directly for the Lincoln Laboratories.

Previous work under Contract DAAA-25-73-C-0256 included several complementary test programs in the millimeter region including: a literature search to locate the available land clutter data above 1 GHz; a test program to determine the radar backscatter properties of rain in the region 10 GHz to 100 GHz; a program to measure the backscatter properties from land clutter in the millimeter region for summer foliage penetration measurements. The results of the programs are summarized in Technical Reports one through four (1, 2, 3, 4).

B. Description of Field Measurements

The goals of this program were to determine the attenuation properties of foliage at millimeter frequencies for summer and winter conditions with the emphasis on high depression angles. Because of logistic and equipment limitations, the approach to the test program involved the use of several field sites and two methods of measuring the penetration properties of foliage. These subjects will be discussed in the following paragraphs.

1. Description of Summer Measurements

Summer foliage penetration measurements were conducted utilizing both one-way and two-way measurement techniques. The one-way measurements were performed at only 9.4 and 16.2 GHz because of lack of remote transmitters at 35 and 95 GHz, while two-way experiments were performed at all four frequencies. A brief description of the two measurement techniques follows.

The two-way experiments were conducted by measuring the attenuation of a radar signal caused by foliage in front of a trihedral corner reflector when the reflector was in a clear unobstructed area, and comparing that level to the level of video recorded when the corner was in an area where the radar view was obstructed by intervening foliage. The difference in the two video levels represented the total two-way attenuation. The corner reflector was first positioned in a clear area, and then moved back into the foliage, in approximately 1 meter increments, until the return from the corner could not be distinguished from the normal clutter returns. The large radar returns from the foliage obscured returns from the corner reflector very quickly so that this method did not allow deep penetrations into the wooded areas.

The one-way experiments provided much deeper penetration into foliage for two reasons. First, since only one path was involved, the attenuation was only half the two-way attenuation. Second, there was no radar return from the foliage to mask the desired received signal as in the two-way case. The one-way measurements were conducted in a manner similar to the two-way measurements except that the corner reflector was replaced by standard gain horns and remote short-pulse transmitters operating at frequencies of 9.4 and 16.2 GHz. Equipment was not readily available to implement the one-way experiment at the higher frequencies so that one-way experiments were not performed at 35 GHz and 95 GHz.

a. Test Sites

The locations of the field sites for the summer measurements were selected after careful investigation of several factors. Boresite declination angle, accessibility for transporting equipment into foliage areas, accessibility, density, and type of trees available were all factors to be considered. Two sites were selected which met the accessibility requirements and offered a variety of foliage types, including both deciduous and coniferous trees. Measurements at depression angles of up to 2 degrees were achievable at Site 1 while a depression angle of 0.4 degrees was available at Site 2. A third site located on the campus of the Georgia Institute of Technology was selected which allowed measurements of a single oak tree at depression angles near 29 degrees. An aerial view of Site 1 is shown in Figure 15. This site is located in the Kennesaw National Battlefield Park. Site 2, also located in the park, was located 1/2 mile northeast of Site 1. The topography of these sites allowed measurements to be conducted in an environment free of multipath effects above a height of 3 meters.

Trees located around Site 1 are typical of forests in North Georgia. Foliage attenuation was measured at five locations around this site. Trees which make up this forest are of the deciduous type and consist primarily of oak, dogwood, hickory, sweetgum and maple. The height of the trees ranged from 4.5 to 21 meters; the smaller trees generally being located near the edges. Figure 16 is a photograph of one of the measurement locations. The distance from the radar van to foliage areas was between 150 and 300 meters. The radars were positioned at the highest point within the field and overlooked an area covered with grass from 10 to 70 cm high. The land sloped down from the position of the radars in three directions with the lowest point being approximately 10 meters below the radar antennas.

Site 2 was near an area containing a grove of young pine trees ranging in height from 3.5 to 8 meters. The largest tree trunk diameter within this pine grove was 19 cm, and the average trunk diameter (within the path of the deepest penetration measurement) was 11 cm. The average tree foliage diameter (total) over this same path was 3 meters. Figure 17 shows this young pine area. The radar van was positioned 106 meters from the pine grove in a hay field which had been cut to a height of 7 cm about 3 weeks



Figure 15. Aerial view of Test Site 1 showing radar van and surrounding foliage areas.



Figure 16. Photograph of typical deciduous tree area near Test Site 1.

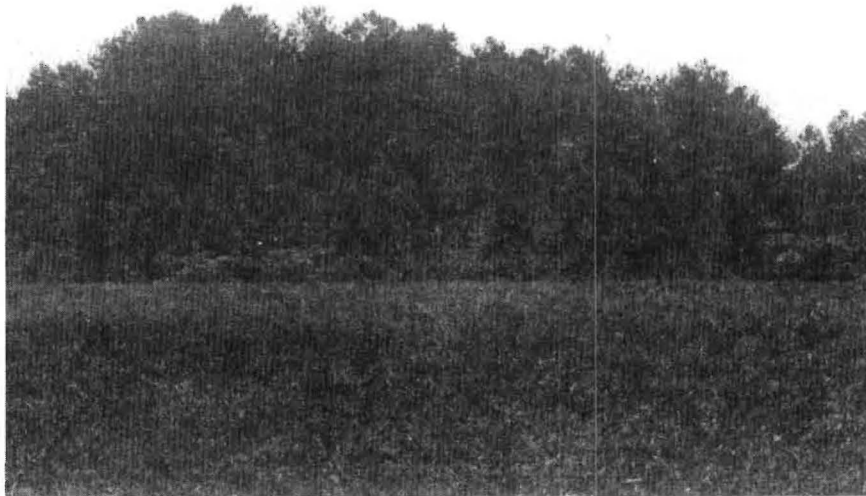


Figure 17. Photograph of young pine grove at Test Site 2.



Figure 18. Photograph of oak tree at Test Site 3.

earlier. The land around the van location was nearly flat for approximately 50 meters, and then very gently sloped down towards the pine grove. Data were also collected on deciduous trees at this site.

Site 3 was located on the Georgia Tech campus. This site was selected because of the large look angle which was available, and because it offered an opportunity to observe a single oak tree and the possibility to repeat the measurements with the tree in a defoliated state during Phase II of the program. Because of the geometry of this site, only one-way attenuation measurements were possible. Figure 18 is a view of the oak tree and the building from which the measurements were made. The measurements were conducted on a weekend to avoid the possible multipath effects caused by parked automobiles. Transmitting equipment was located on the roof of the building at a distance of 47 meters from the radar van. The geometry of this site is shown in Figure 19. The radar van was moved laterally along a straight line from a clear reference point to 8 different positions behind the tree while the received signal levels were recorded at each position. Attenuation coefficients were measured for both horizontally and vertically polarized transmitted signals.

b. Instrumentation Radars

The four instrumentation radars used for the summer measurements are mounted in a single test vehicle along with integrated controls and data-acquisition equipment, as shown in Figure 20. The 9 GHz, 16 GHz, and 35 GHz radars are permanently mounted in the test vehicle with removable antennas on the roof. In order to minimize waveguide losses, the 95 GHz radar is integrated into a single package and sits on a platform on the van roof. The boresight angle of each antenna is capable of being individually positioned in both the azimuth and elevation planes. Parameters of the radars are given in Tables 3 through 6. Although the I-Band and J-Band systems can be tuned over a range of frequencies, they were set for these tests at 9.4 and 16.2 GHz, respectively.

While differing in detail, the 9, 16, and 35 GHz radars are generally similar. They are all short-pulse systems with dual-polarized antenna feeds; that is, they receive both horizontal and vertical polarizations simultaneously while transmitting either horizontal or vertical polarization. These three systems may be operated in either the scanning or

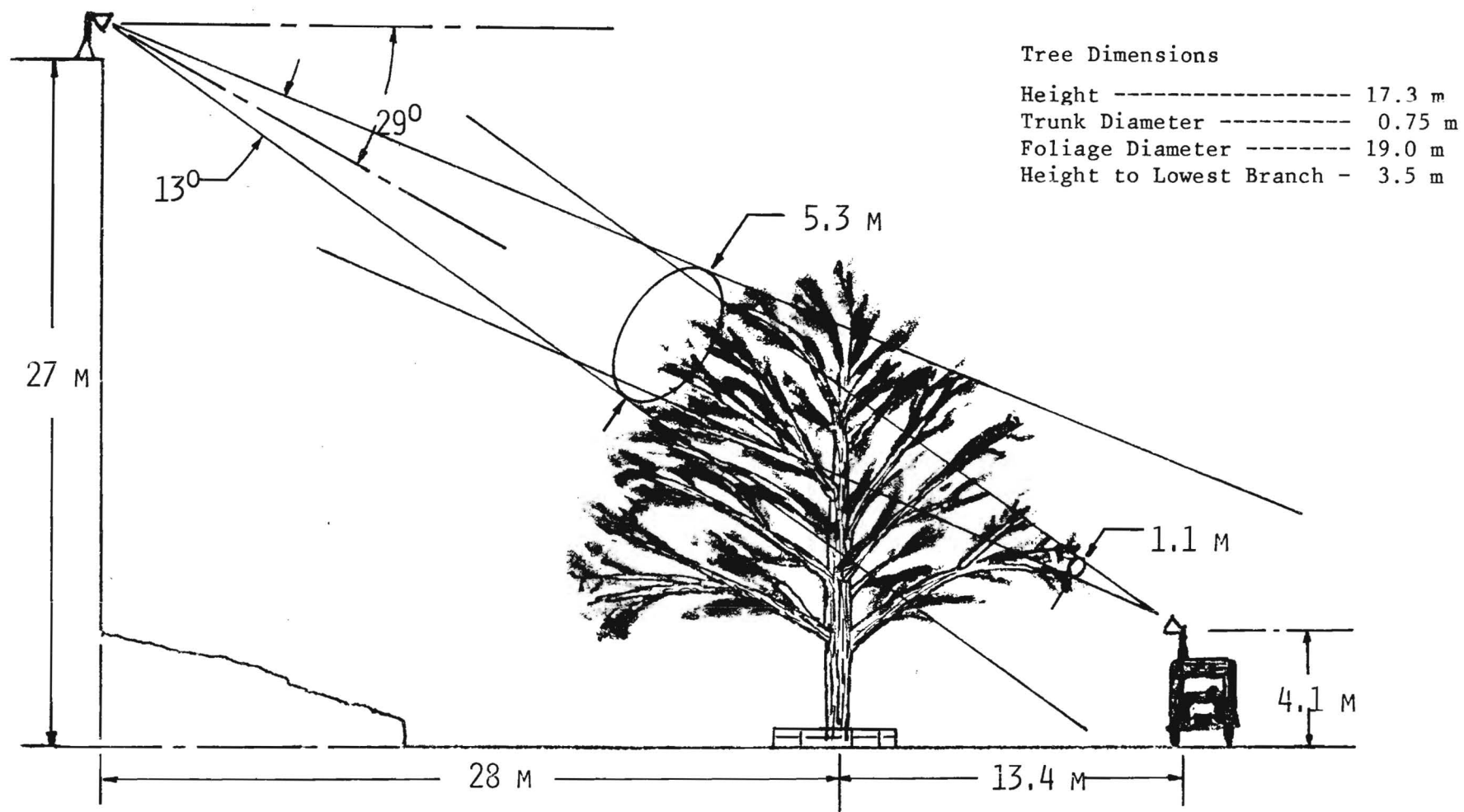


Figure 19. Geometry of one-way large depression angle experiment.

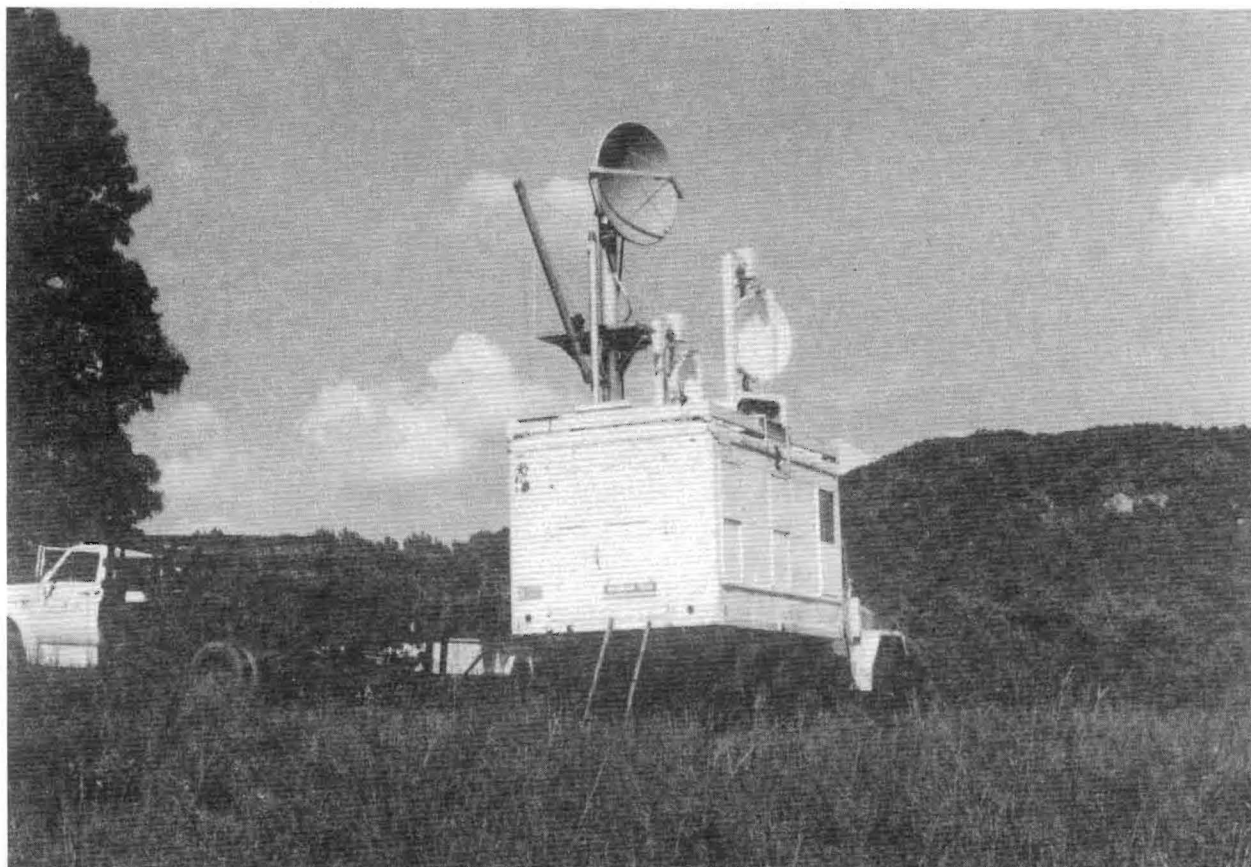


Figure 20. Photograph of test radar van located at Test Site 1.

Table 3
PARAMETERS OF GEORGIA TECH GT-I EXPERIMENTAL RADAR

<u>Parameter</u>	<u>Description</u>
Frequency	8.5-9.6 GHz
Peak Power	40 kW
Pulse Width	50 ns
PRF	0-4000 pps
Antenna Type	Nonscanning Paraboloid
Azimuth Beamwidth	1.5°
Elevation Beamwidth	1.65°
Antenna Gain	Vertical Polarization 41.4 dB Horizontal Polarization 41.6 dB
Antenna Type	Scanning Parabolic Cylinder
Scan Rate	0-100 RPM
Azimuth Beamwidth	2°
Elevation Beamwidth	5°
Antenna Gain	Vertical Polarization 30 dB Horizontal Polarization 31 dB
Polarization	H or V transmitted H and V received simultaneously
IF Center Frequency	60 MHz
IF Bandwidth	20 MHz
IF Response	Logarithmic (linear available)
Noise Figure	12 dB
Dynamic Range	80 dB
Display Type	A-scope

Table 4
PARAMETERS OF GEORGIA TECH GT-J EXPERIMENTAL RADAR

<u>Parameter</u>	<u>Description</u>
Frequency	16-17 GHz
Peak Power	50 kW
Pulse Width	50 ns
PRF	0-4000 pps
Antenna Type	Scanning Paraboloid
Scan Rate	0-120 rpm
Azimuth Beamwidth	1.5°
Elevation Beamwidth	1.5°
Antenna Gain	Vertical Polarization 41.5 dB Horizontal Polarization 41.4 dB
Polarization	H or V transmitted H and V received simultaneously
IF Center Frequency	60 MHz
IF Bandwidth	20 MHz
IF Response	Logarithmic (linear available)
Noise Figure	13 dB
Dynamic Range	70 dB
Display Type	A-scope, B-scope, PPI

Table 5
PARAMETERS OF GEORGIA TECH GT-K EXPERIMENTAL RADAR

<u>Parameter</u>	<u>Description</u>
Frequency	35 GHz
Peak Power	40 kW
Pulse Width	50 ns
PRF	0-4000 pps
Antenna Type	Scanning Paraboloid
Scan Rate	0-120 rpm
Azimuth Beamwidth	1°
Elevation Beamwidth	1°
Antenna Gain	Vertical Polarization 43 dB Horizontal Polarization 43 dB
Polarization	H or V transmitted H and H received simultaneously
IF Center Frequency	60 MHz
IF Bandwidth	20 MHz
IF Response	Logarithmic (linear available)
Noise Figure	14 dB
Dynamic Range	70 dB
Display Type	A-scope, B-scope, PPI

Table 6
PARAMETERS OF GEORGIA TECH GT-M EXPERIMENTAL RADAR

<u>Parameter</u>	<u>Description</u>
Frequency	95 GHz (Nom)
Peak Power	6 kW
Pulse Width	50 ns or 10 ns
PRF	0-4000 pps
Antenna Type	Paraboloid (Cassegrain)
Azimuth Beamwidth	.70 ^o
Elevation Beamwidth	.65 ^o
Antenna Gain	Vertical Polarization 46.3 dB Horizontal Polarization 46.3 dB
Polarization	H or V
IF Center Frequency	60 MHz or 160 MHz
IF Bandwidth	20 MHz or 100 MHz
IF Response	Logarithmic (linear available)
Noise Figure	15 dB
Dynamic Range	70 dB
Display Type	A-scope

nonscanning mode. The 9 GHz radar has both a 3-foot scanning parabolic cylinder and a 5-foot diameter nonscanning paraboloidal dish. Each antenna is equipped with boresight telescopes rigidly mounted to the antenna feed support. All three of these systems incorporate logarithmic receivers of wide dynamic range (approximately 80 dB) to permit accurate measurement of returns from targets having a widely varying signal strength. Each system incorporates provisions for injecting a known calibration signal into both parallel- and cross-polarized channels. A common prf reference of 2000 Hz was used for all systems during the tests described here. A simplified block diagram typical of the radars used for these measurements is shown in Figure 21.

The 95 GHz system is somewhat different from the other three systems in that the antenna is a nonscanning Cassegrain type and all controls are mounted in one package containing antenna, transmitter, and receiver. A boresight telescope is also provided for accurately positioning the antenna. Although the antenna has a dual-polarized feed, only one receiver channel is currently incorporated.

The antenna sizes of the four radars resulted in beamwidths ranging between 1.5 degrees for the 9.5 GHz radar (2.0 degrees with the scanning parabolic cylinder) to 0.7 degrees for the 95 GHz radar. Figure 22 gives a close-up of the four antennas on the top of the radar van.

c. Remote Transmitters

To accomplish the one-way attenuation measurements, signal sources were required at the remote (target) site to transmit short pulses of energy to the receivers located in the radar van. These signals were provided by two low-power radar transmitters operating at 9.4 and 16.2 GHz, respectively. Parameters for the remote transmitters are given in Table 7. Synchronization between the remote equipment and the data-acquisition equipment was achieved by transmitting a short pulse at 9 GHz from the radar van. This pulse was detected, amplified and used to generate a trigger for the two remote transmitters. A block diagram of

DUAL-POLARIZED
ANTENNA

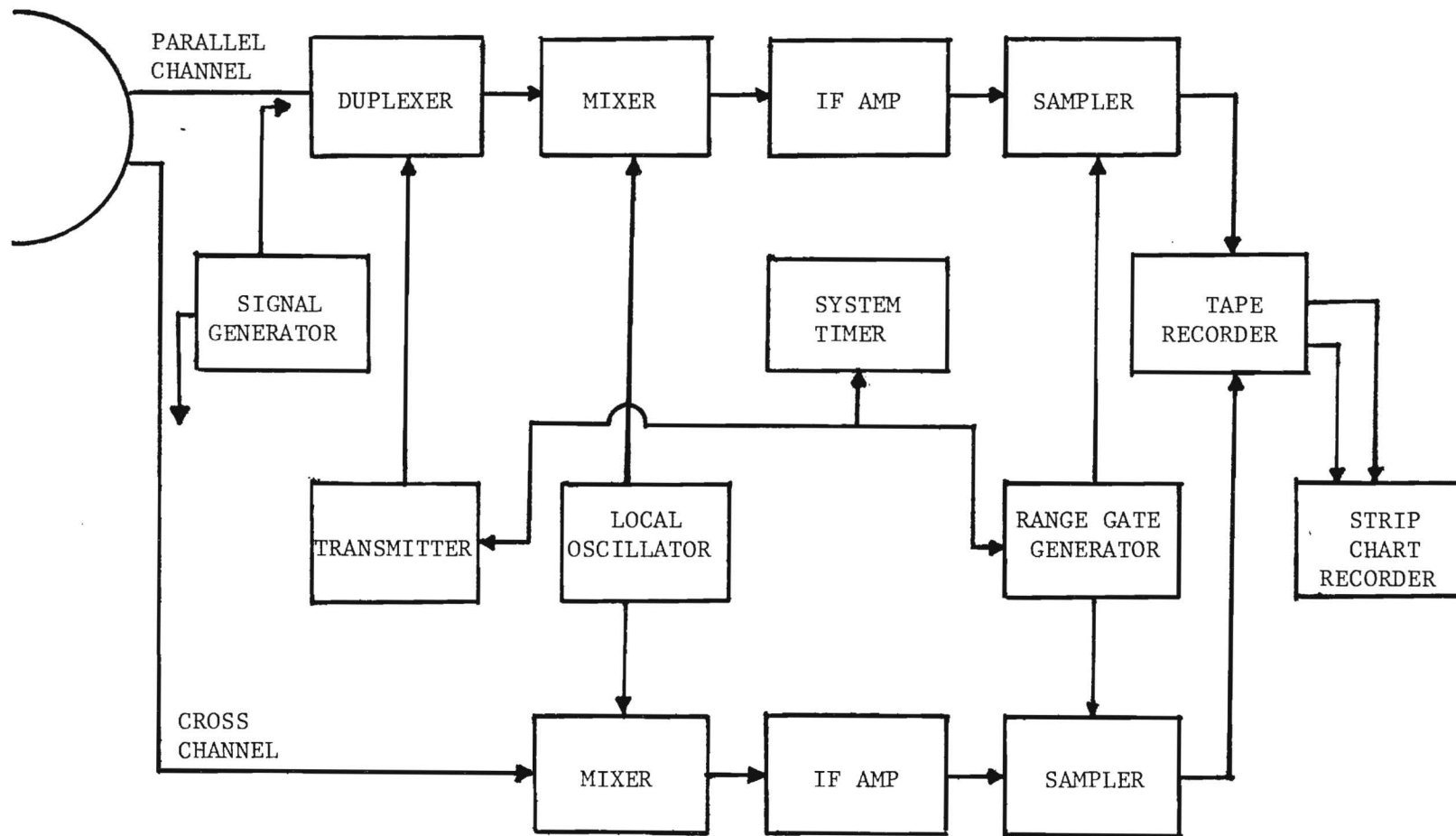


Figure 21. Simplified block diagram of equipment configuration of typical instrumentation radar.

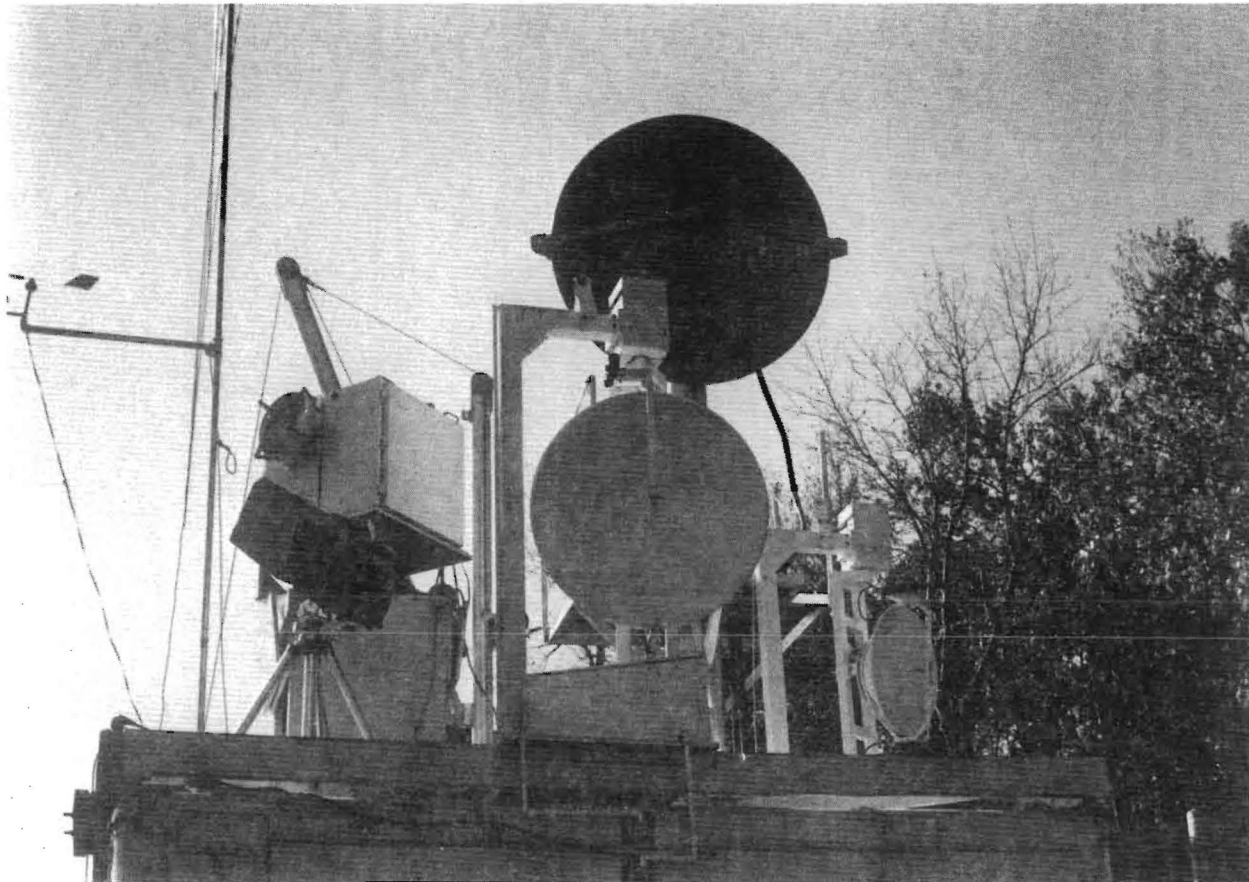


Figure 22. Close up view of radar antennas.

TABLE 7
PARAMETERS FOR REMOTE TRANSMITTERS

<u>Parameter</u>	<u>Description</u>	
Type	Pulsed Magnetron	
Modulator	Lumped Constant Delayline/Thyratron	
Frequency	9.4 GHz	16.2 GHz
Pulse Width	50 nsec	80 nsec
Peak Power	8 kW	8 kW
PRF	2000 Hz	2000 Hz
Antenna	SGH-8.20	SGH-12.4

the equipment configuration used in the one-way measurements is shown in Figure 23. Signals from the remote locations were transmitted to the radar van through standard gain horns.

A photograph of the remote transmitters and synchronizing equipment used in the one-way attenuation measurements is shown in Figure 24.

d. Signal Conditioning and Recording Equipment

The rf energy received by the radar antennas is converted to an intermediate frequency in balanced mixers fed with local oscillators operating at frequencies 60 MHz below the received signal. The 60 MHz if signals are amplified and detected in RHG type LST 6020 logarithmic amplifiers. The resultant log video is buffered by line drivers before being routed to the various signal conditioning and monitoring equipment. Dual-mode couplers are incorporated into each antenna so that the two polarization components, one parallel - to and one orthogonal - to the polarization of the transmitted wave, are received. The two polarization components of the channels for the received signals are simultaneously processed through independent receivers of the 9, 16, and 35 GHz radars. (The 95 GHz radar is not presently configured for dual polarization.)

A console inside the radar van provides the operator easy access to radar controls, displays, and data-acquisition equipment. Located at the console are two A-scope displays, a B-scope display, a frequency counter and radar timing circuitry, and a six-channel narrow-aperture video sampler. The video sampler is used to sample, with a 30 nanosecond aperture, at a given range, the radar video from each of the six channels, and hold the sampled value for one interpulse period. Amplitude data at the output of the video samplers are recorded on a 7-channel fm tape recorder with a dynamic range of approximately 40 dB. Typically four channels of the range gated and stretched video are recorded simultaneously along with a voice track, a sample synch pulse, and a time code signal. This allows the parallel channels at all four frequencies to be recorded simultaneously or parallel and cross channels at two frequencies to be recorded simultaneously.

The radar transmitter controls and rf signal generators are located in a rack to the left of the operator's console. The signal generators

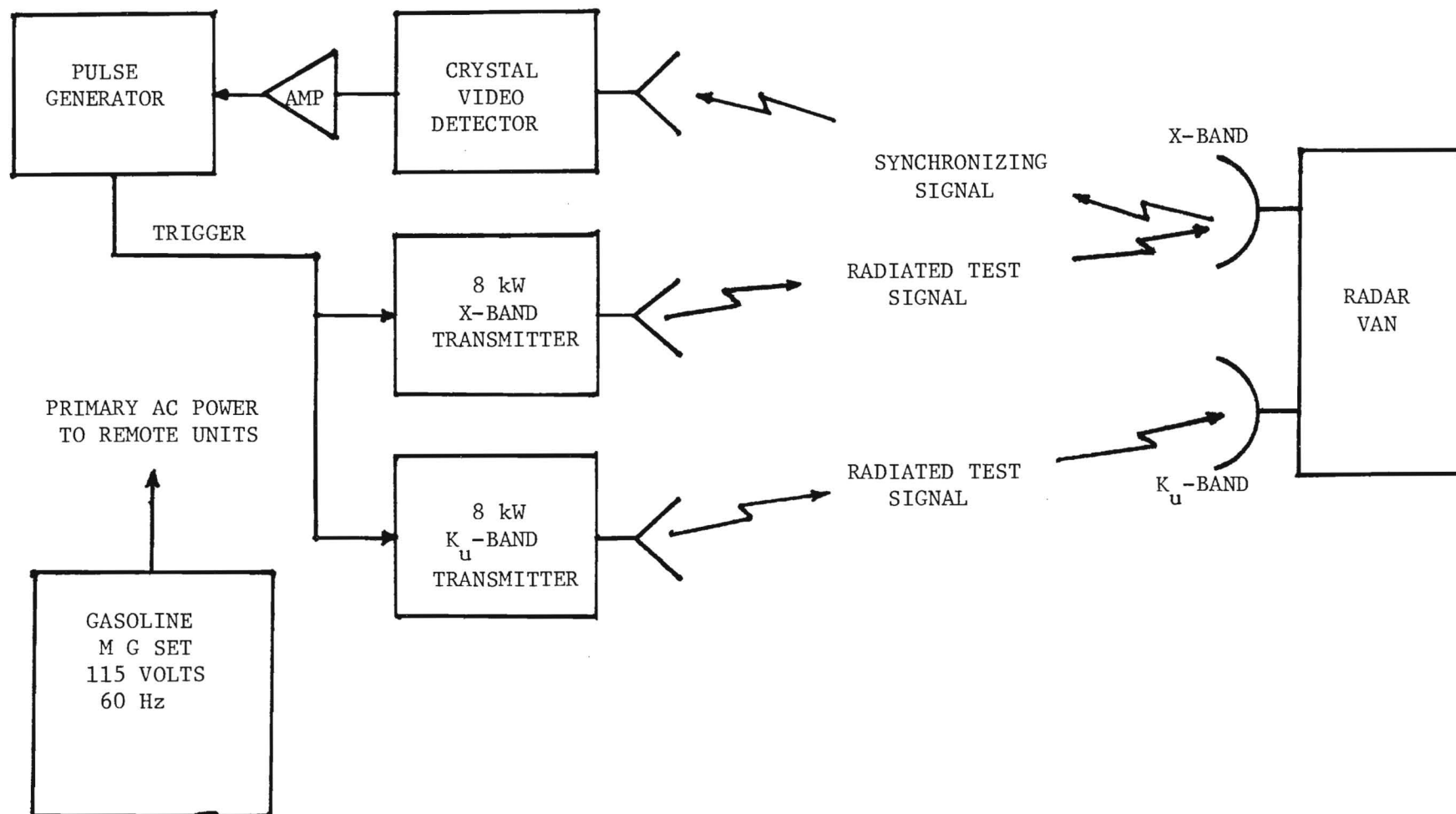


Figure 23. Block diagram of equipment configuration used in one-way measurements.



Figure 24. Remote transmitters and transmitting horns used in one-way experiments.

are used to calibrate the 9, 16, and 35 GHz radar receivers by injecting known rf signal levels into directional couplers installed in the waveguide between the antenna and the receiver mixers. The receiver calibration or transfer function is generated by attenuating the injected signal level in 10 dB increments from 0 dB through the receiver noise level and recording the sampled video on magnetic tape. Signal losses between the receiver inputs and the directional coupler are added to the calibration levels in the data-reduction program in order to determine the received power level at the receivers.

A signal generator is not available to calibrate the 95 GHz radar. Calibration of this system is achieved by placing a corner reflector of accurately known radar cross section in front of the radar. A receiver transfer function is generated by varying an rf attenuator in 10 dB steps as was done for the other radars. Calibrations achieved in this manner are directly related to the radar cross section of the reference corner reflector and yield accurate results if site-dependent factors are taken into consideration.

e. Measurement Procedures

The collection of radar data requires that careful attention be directed towards developing a set of procedures and definitions which will adequately present a proper framework for interpretation. Although the primary concern here is for the attenuation factor, which is a relative quantity, full calibration procedures were followed so that the data obtained here could be analyzed for backscatter coefficients, etc, if desired. A careful test procedure was routinely followed and ensured a high degree of confidence in the numerical value of the raw data. However, specific problems associated with foliage definition, near-field effects, and multipath effects had to be addressed before a fully satisfactory procedure could be developed which would lead to confidence that the data are truly representative of the actual foliage attenuation.

Preliminary experiments were conducted at the field site to determine a satisfactory criterion by which foliage depth could be measured. Several experiments were conducted in which a corner reflector or a signal source was placed in a clear area and then moved back into a

foliated area. The differences between the signal levels received at the radar for the two conditions were calculated. This difference represents the total attenuation of the signal due to the added foliage and when divided by the path length is the attenuation coefficient with units of dB/unit length. After several experiments at various depths into the foliage, it was determined that the measure of foliage depth which led to the least variability in the attenuation coefficient was a summation of the actual measured depth of each individual tree branch in the signal path. This criterion not only led to the least variability in the data, but also led to good agreement between the one-way and two-way measurements.

The effects of multipath had to be considered before measurements were made, since the corner reflector or sources had to be moved during these experiments. Radiated waves propagating over different paths and arriving at the same point vectorially sum to create nulls and lobes in the energy field. To determine if ground reflections were a problem, a field probe was placed at the clear measurement location. Figure 25 illustrates the effect of ground reflections at the measurement site. The field probe was a 4-meter-high aluminum pole with a corner reflector attached to a motor-driven mount which was uniformly raised in height above the ground while the return power at the radars was measured. The measured power at the radars was found to be constant above a height of 3 meters at the four measurement frequencies.

Near-field effects were noticed when intervening foliage was near the corner reflector or horn antennas. These effects were verified experimentally by placing cut branches at various distances in front of the corners and horns and measuring the received power. Large variations in received power were present when the foliage was located within one meter of the corner or horns. At a distance of 3 meters, power variations were sufficiently small so as to be attributed to movement within the foliage rather than disturbances within the near-field region of the horns. The near-field distance based on the horn dimensions is approximately 2.5 meters. The dimensions of the corner reflectors (up to 55 cm) used in the experiments were so large that a far-field criterion could not be met, in all cases, because of the natural environment in which the experiments

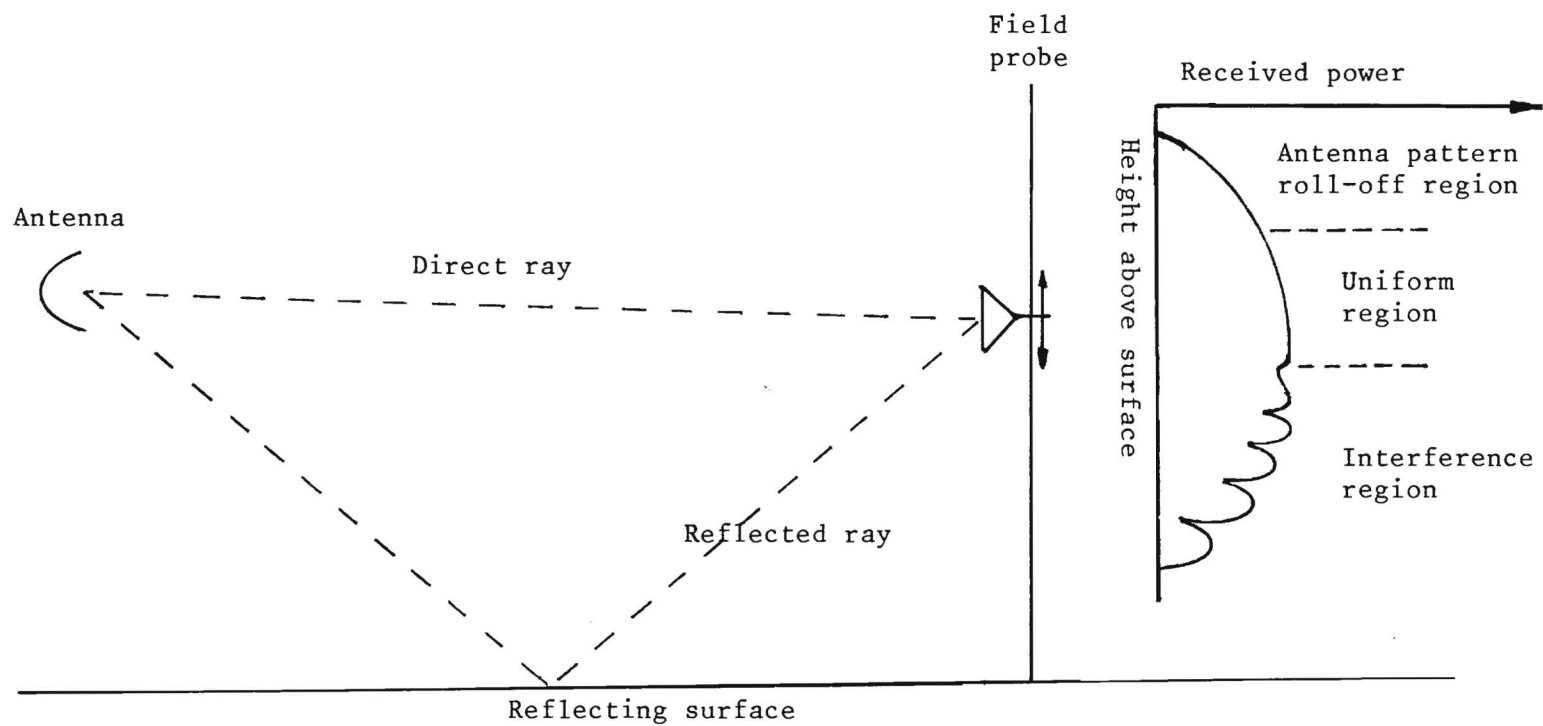


Figure 25. Illustration of the effect of ground reflections on the field pattern of the radar. The maximum height of the interference region was 3 meters above the surface.

were conducted. Meeting the far-field criterion is perhaps academic for these measurements, since, among other things, the foliage itself may be considered a new source of radiation with extremely large dimensions, resulting in a non-uniform phase front out to great distances. In addition, targets, such as vehicles, located under a tree canopy will normally have sufficiently large dimensions that the near field of the reflected wave will extend beyond the canopy. In these experiments, however, the far-field criterion was generally satisfied for the one-way measurements, and as much distance as possible was allowed between the foliage and the corner reflector for the two-way measurements.

Based on the results of these preliminary experiments, a set of procedures to be followed in setting up the remotely located equipment was established. In setting up the remote equipment, all locations in the foliage were marked on a radial path between the clear reference point and the radar van. In the two-way experiments, measurements were made at three lateral locations spaced approximately 1/3 meter apart at each foliage depth. In the one-way experiments, measurements were made at the three lateral locations and also at heights of 3, 3.4, and 3.8 meters. This procedure allowed either three or nine samples over the same general foliage path for the one-way and two-way experiments, respectively. Video samples of the signals were recorded for one minute at each location.

2. Description of Winter Measurements

The winter measurements were carried out in the same manner as the summer measurements except that because of limitations in available funds, one-way measurements only were performed at Test Site 3. The same techniques for the one-way measurements were used for winter and summer measurements so that the results could be directly compared.

a. Test Site

Test Site 3 was selected for the winter measurements because it offered the possibility of readily taking winter measurements at a high depression angle through precisely the same beam paths through which some of the summer measurements had been made. Figure 26 shows the view of the transmitter site from the receiving antenna looking through the defoliated oak tree. Because of the tendency of tree leaves to face the sun, foliage

will be concentrated on the upper and outer layers of a tree and thus the expected attenuation will be larger at higher angles of incidence, up to about 45 degrees. Accordingly, the differences between summer and winter attenuations should be greatest for beam paths of higher depression angles. Site 3, with a depression angle of about 29 degrees, thus offered the best opportunity to estimate the effects on attenuation contributed by the deciduous leaves alone. The higher depressions angle also affords a more realistic simulation of the mini-RPV case.

b. Instrumentation Radars

The winter measurements were performed using the 9.4 and 16.2 GHz radars only, and the one-way technique. As shown previously in Figure 19, the remote transmitters were positioned atop a building at a slant range of 47 meters from the receivers which were located on the radar van. The performance parameters of the radars and remote transmitters are found in Tables 3, 4, and 7. Because of the background at Site 3 two-way measurements were not practicable, and the one-way measurements were conducted on a weekend to avoid possible multipath interference by parked automobiles. The radar van with the receiving antennas, which is shown in Figure 27, was moved laterally along a straight line from a reference point in the clear to 5 different positions behind the tree. The van tire positions were marked with paint on the parking lot surface during the summer measurements to permit exact repositioning of the van during the winter measurements.

c. Measurement Procedures

The test procedure followed for the winter measurements were as similar to the procedure for the summer measurements as was practical. The same site, radars, data gathering equipment, and personnel were used, and as stated previously, the instrument van was positioned at the same spots as for the summer measurements so that the portions of the tree penetrated by the radar beams were very close to the same. By this technique, it was hoped to be able to directly compare the results for the foliated and defoliated states, and thus determine the effects of the foliage on the penetration properties.



Figure 26. View of the transmitter site from the receiving antennas looking through the defoliated oak tree.



Figure 27. View of the radar vans and receiving antennas used for the winter measurements.

6. DATA RESULTS

A. Data Analysis Techniques

The data obtained from the radar penetration measurements consisted primarily of fm magnetic tape recordings of amplitude fluctuations of the received signals from the remote transmitters or corner reflectors for the one-way and two-way experiments, respectively. Strip chart recordings, A-scope photographs, and other miscellaneous data such as log sheets of wind-speed and direction, provided background information to supplement the magnetic tapes, but were not analyzed directly.

1. Data-Reduction Facility

Data-reduction facilities of the Advanced Sensors Division of EES were used to process the magnetic tapes from the radar foliage penetration tests. These include the following: (1) an analog signal-conditioner unit which provides variable gain and offset to allow the interface of varied tapes of signals to the data-reduction facility; (2) a Fabri-Tek Model 1072 Instrument Computer which serves as an A/D and D/A interface, and also computes real-time pulse-height distributions. The D/A output from the Fabri-Tek computer can be displayed on a CRT display or can be plotted on an x-y plotter; (3) a PDP-8/F computer which can exchange information directly with the Fabri-Tek computer; (4) a teletype; and (5) a Digital Equipment Corporation Decassette Recorder for program development and storage.

The PDP-8/F computer contains 16K of memory, of which 8K is magnetic core. An extended version of FOCAL_{TM} has been developed for use with the PDP-8/F and is designated FOCL/F. This language is interactive and greatly facilitates program correction and modification. Also available is an in-house developed machine language software package for calculating fast Fourier transforms (FFT), and a set of software commands for Fabri-Tek control. These two machine language software packages, along with the extended FOCAL_{TM} software, make this system a very powerful and flexible data-reduction facility.

2. Data Analysis Procedure

Pulse-height amplitude distributions are calculated by the data facility and are displayed in two forms: as probability density plots

and as probability distribution functions. The probability density plots are generated from data time histories from the magnetic records. The analyzer samples the input analog time history, A/D converts the samples, determines into which of 1024 amplitude bins the sample belongs, and increments a stored variable corresponding to the number of samples which have fallen in that amplitude window. When repeated a large number of times, this process generates a voltage amplitude distribution which is then calibrated and divided by the total number of samples to achieve a normalized probability density function. Approximately 30 seconds of data were used to generate the distributions analyzed resulting in about 60,000 samples. Assuming a decorrelation time of 50 milliseconds at X-Band, this results in about 6000 independent samples for the worst case.

The voltage amplitude distributions are calibrated by reference to a known comb (amplitude) signal. The peak of the distribution for each voltage step in the calibration comb is assigned the dB value corresponding to that calibration step. The PHA program in the PDP-8/F then does a cubic fit to the calibration and generates an equation relating dB value and amplitude bin number. The cubic fit program was developed to "linearize" non-uniform calibration steps so that the output density functions can be plotted on a linear scale.

The probability distributions are calculated by point-to-point numerical integration of the probability density functions. The functional values of these distributions are then multiplied by a nonlinear transfer function so that they can be plotted on probability paper.

The resultant probability distributions are useful in determining the median values of the distributions and also their shapes. In addition, for certain classes of functions, the average values can be determined from the distributions using a simple formula.

B. Summary of Results

1. Interpretation of the Data

The new foliage penetration data presented in this report was obtained for defoliated conditions at only one depression angle and for only two frequencies due to funding limitations. Thus, it is not possible to determine the frequency dependence of the attenuation coefficient as was done for the case of the summer foliage penetration data (since the attenuation

constant was determined at only two frequencies). However, since the winter measurements were performed at one of the same sites, it was possible to determine the effects of the foliage alone on the propagation through the tree canopy. Great care was taken to be sure that the same parts of the oak tree at Site 3 were penetrated for both the summer and winter measurements so that the results could be compared directly.

One of the most serious difficulties encountered during the summer measurement program was the problem of developing a suitable definition of foliage depth. As is obvious from examining a tree, its foliage canopy is not uniform, being grouped into branches often with large open areas between the branches. Also, the outside layers of foliage of a tree tend to be more thickly foliated because of the absence of sunlight in the interior parts of the tree. In addition, within a given branch, the location of the foliage and limbs can be very non-uniform, and most certainly the uniformity varies with tree type.

After some experimentation, it was determined that a foliage definition based on layers of foliage in the path of the radar beam works fairly well. For this definition, the foliage thickness is computed by determining the number of branches or foliage layers in the beam path, measuring the gross thickness of each layer, and summing the depths of the various layers to obtain the total thickness. The non-uniformity of the layer densities are ignored because of the difficulties in determining these densities. Obviously, since individual branches on a tree and also different trees do have different foliage densities, there are some errors in the foliage depth estimates using this method. However, it was determined that the spread in the foliage attenuation coefficients measured caused by the inability to characterize the foliage densities exactly was less than a factor of two-to-one for a very densely foliated branch as opposed to a very light one. It was also noticed that differences in the attenuation coefficient measured for individual branches on a given tree were greater than the average differences between types of trees including deciduous and coniferous trees.

For the winter measurements, the same foliage depths were assumed as were used for the summer measurements. Otherwise, it would be very difficult to determine foliage depth from just the bare limbs. By using

the same foliage depths for the summer and winter cases, the differences in attenuation coefficient will reflect only differences due to the presence or absence of the foliage thus accenting the effects of the foliage on the attenuation of the tree canopy.

Previous measurements of foliage attenuation have been concentrated in the frequency region 50 to 3,000 MHz, with the primary emphasis on propagation of one-way television and communications transmissions. Also, many of the experiments have been performed with CW equipment so that their applicability to the high-frequency pulsed-radar case is in doubt. Moreover, foliage depth has been determined by measuring the line-of-sight distance through a forest, ignoring spaces between trees and spaces between the tree limbs, a procedure which results in obvious problems in obtaining consistent values of the attenuation constant.

However, the results of some of these low-frequency experiments can be used to estimate "ball park" values for attenuation for the higher frequency pulsed radar case. Nathanson has derived an equation for attenuation compiled by Saxton and Lane which is given by: (9, 10)

$$A(\text{dB/m}) = 0.25 f^{3.4}$$

where f is in GHz.

This would yield values for the attenuation coefficient of 0.25 dB/m at 1 GHz, 1.4 dB/m at 10 GHz and 7.9 dB/m at 100 GHz. The foliage depth estimates for these measurements were based on the line-of-sight distances through a foliated forest, and thus result in lower values for the attenuation coefficient than the definition used for the present penetration measurements (foliage layers). However, Nathanson's equation compared well with the new data obtained under the first phase of this program if the asymptotes of the attenuation versus depth curves were used as the attenuation coefficient values. (8) The attenuation coefficients calculated using the two different definitions of foliage depth can be approximately related if it is assumed that a given forest is approximately 50% foliage and 50% open space. Thus, the equivalent attenuation values given by Nathanson's equation would be approximately half as great as the attenuation constants determined using the foliage layer definition.

2. Penetration Data Summary

The results from the winter foliage penetration measurement, along with a summary of the summer measurements, are given in this section. As stated previously, the winter measurements were very limited in nature, consisting of data at one site and two frequencies only. All penetration values discussed, whether derived from one-way or two-way experiments, are expressed in terms of the one-way foliage depth.

a. Results of Summer Measurements

Most of the data obtained during the summer represented measurements taken at depression angles of less than 3 degrees. Because of the large total depth of the forest foliage canopy at the greater depression angles, the two-way measurements had to be made at a tree line where only small grazing angles of depression could be achieved. However, one-way measurements were performed at the same sites as the two-way measurements and were also performed for a high depression angle situation.

Table 8 gives a summary of the one-way low angle summer data. The median values of attenuation coefficient were about 2.6 dB/m at X-Band and 3.5 dB/m at Ku-Band. The mean values were slightly higher and horizontal polarization was higher than vertical for X-Band, and vertical was higher at Ku-Band. The two-way attenuation results (low angle) are summarized by Table 9. Median values for the attenuation coefficient varied from approximately 2 dB/m at 9.4 GHz to 3.6 dB/m at 95 GHz. The mean values were once again slightly higher, and no polarization trend was observed for the different frequencies. The large depression angle measurements (summer) are summarized by Table 10. Note that the median values of attenuation coefficient are higher than the low depression angle data. This is most likely due to the greater foliage depths penetrated, since it was found that the measured attenuation coefficient increases with foliage depth approaching asymptotically a constant value.

TABLE 8
SUMMARY OF ONE-WAY
ATTENUATION MEASUREMENTS
FOR SITES 1 AND 2
(SUMMER)

Polarization	9.4 GHz		16.2 GHz	
	V	H	V	H
Median Attenuation Coefficient (dB/m)	2.6	2.7	3.7	3.3
Mean Attenuation Coefficient (dB/m)	2.7	3.1	3.8	3.5
Standard Deviation (dB/m)	0.7	1.4	1.2	1.1

TABLE 9
SUMMARY OF TWO-WAY ATTENUATION MEASUREMENTS (SUMMER)

Frequency	9.4 GHz		1.62 GHz		35 GHz		95 GHz
Polarization	V	H	V	H	V	H	V
Median (dB/m)	1.9	2.3	2.7	3.1	3.4	3.3	3.9
Mean (dB/m)	2.0	2.5	2.7	3.5	3.7	3.0	4.1
Std. Deviation (dB)	0.84	0.61	0.76	1.10	0.30	1.56	1.30

TABLE 10
LARGE DEPRESSION ANGLE MEASUREMENTS (SUMMER)

	9.4 GHz	16.2 GHz
Median Attenuation Coefficient (dB/m)	3.25	4.15
Mean Attenuation Coefficient (dB/m)	3.39	4.17
STd Deviation (dB/m)	.40	.42
Mean Attenuation over Path (dB)	19.87	22.4
Mean Path Length (m)	15.60	15.7
Mean Foliage Depth (m)	5.79	5.44
Loss Per Meter on Mean Path Length (dB/m)	1.27	1.43
Loss Per Meter Based on Mean Foliage Depth (dB/m)	3.43	4.12

b. Results of Winter Measurements

The winter data were all obtained for the high depression angle case. Table 11 gives a summary of the results. Median values of 1.6 dB/m were obtained at X-Band, and median values of 1.8 dB/m were obtained at Ku-Band. These values were approximately half of the values obtained under summer conditions as shown by Table 12, which gives the average value of attenuation coefficient obtained at each foliage depth for summer and winter conditions. This is further illustrated by Figures 28 and 29, which give a plot of the summer/winter attenuation coefficients measured as a function of foliage depth for X-Band and Ku-Band respectively. These plots illustrate that the defoliated canopy attenuation is approximately half of the foliated canopy attenuation.

Figure 30 gives a summary of the summer high/low depression angle data and the winter high depression angle data as a function of frequency. Also plotted on the graph is Nathanson's equation for attenuation coefficient (solid line) and Nathanson's equation corrected for the difference in the foliage depth definition (broken line with dots). The dashed line is a least squares fit to the summer low angle data, and the circles represent the asymptotic values of the low angle data for large foliage depths. Finally, the squares fit to the summer low angle data, and the circles represent the asymptotic values of the low angle data for large foliage depths. Finally, the squares are the high angle summer values and the triangles are the high angle winter values. The summer data appears to fit Nathanson's equation (corrected for foliage depth definition) for large foliage depths and the winter data appears to fit Nathanson's equation uncorrected, although this is not certain since values of attenuation coefficient were obtained for only two frequencies.

Figures 31 and 32 give probability distributions of the power received through the water oak tree for two foliage depths and winter/summer conditions at 9.4 GHz and 16.2 GHz. There is little difference in the width of the power distributions for the winter versus the summer case indicating that most of the fluctuations in the transmitted power are due to the movement of limbs blocking the transmitted beam path rather than to changes in the amount of foliage in the beampath as the wind blows. It should also be

TABLE 11
LARGE DEPRESSION ANGLE MEASUREMENTS (WINTER)

	9.4 GHz	16.2 GHz
Median Attenuation (dB/m)	1.58	1.81
Mean Attenuation Coefficient (dB/m)	1.57	1.72
STd Deviation (dB/m)	.32	.66
Mean Attenuation over Path (dB)	8.36	9.60
Mean Foliage Depth (m)	5.36	5.32
Loss Per Meter Based on Mean Foliage Depth (dB/m)	1.56	1.34

TABLE 12
SEASONAL ATTENUATION COEFFICIENT CHANGES OVER
SPECIFIC RADAR BEAM PATHS

9.4 GHz

	Path Length (m)	Summer (dB/m)	Winter (dB/m)	Δ (dB/m)
1.	3.9	3.00	1.70	1.3
2.	4.2	3.12	1.52	1.6
3.	6.0	3.20	1.55	1.65
4.	6.25	3.84	1.96	1.88

16.2 GHz

1.	3.9	4.75	0.96	3.79
2.	4.2	4.26	1.66	2.60
3.	6.0	4.17	1.97	2.20
4.	6.25	3.81	2.02	1.79

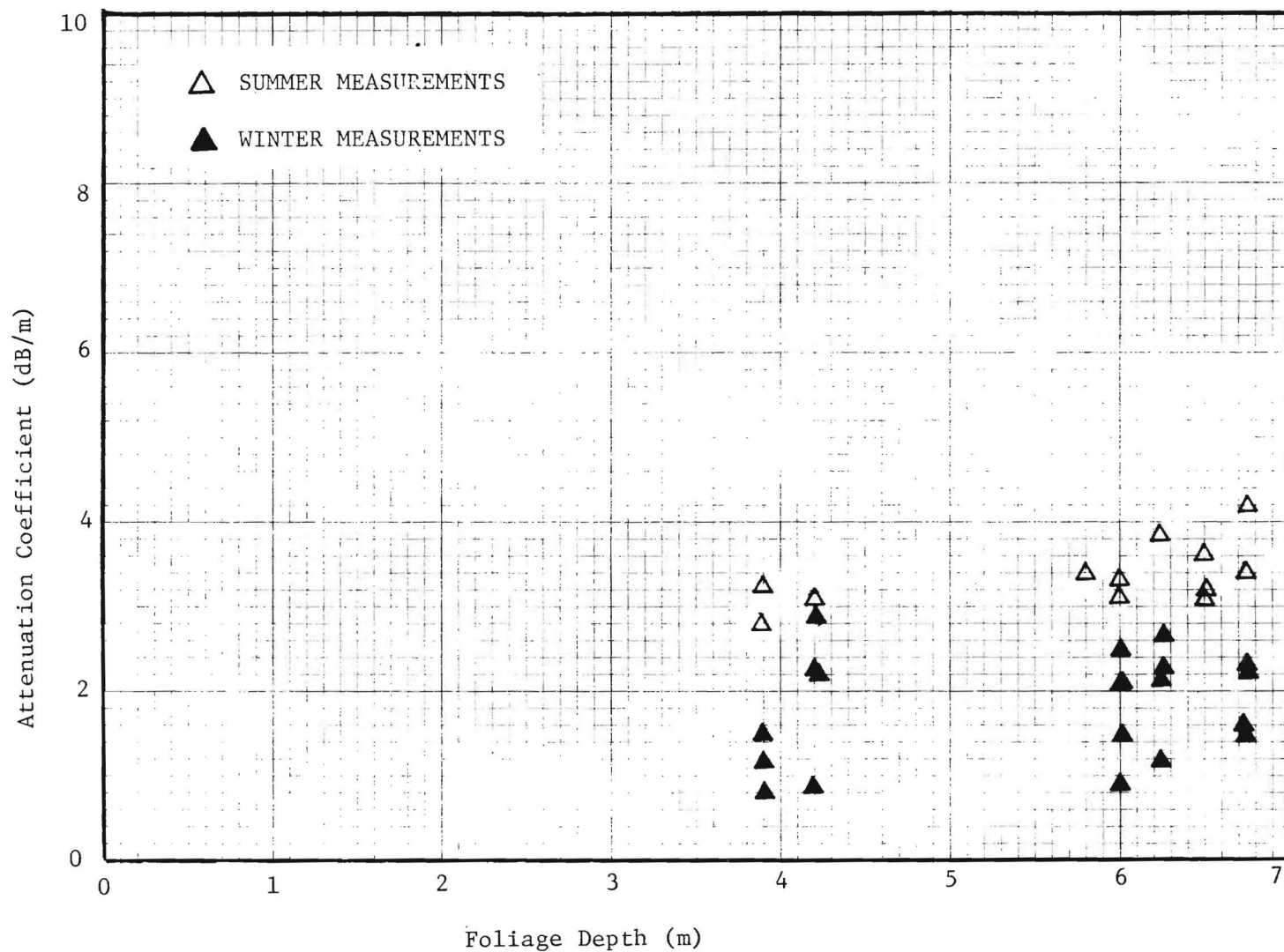


Figure 28. Comparison of the summer/winter values measured for the foliage attenuation coefficient of a water oak tree as a function of foliage depth, 9.4 GHz, 29° depression angle.

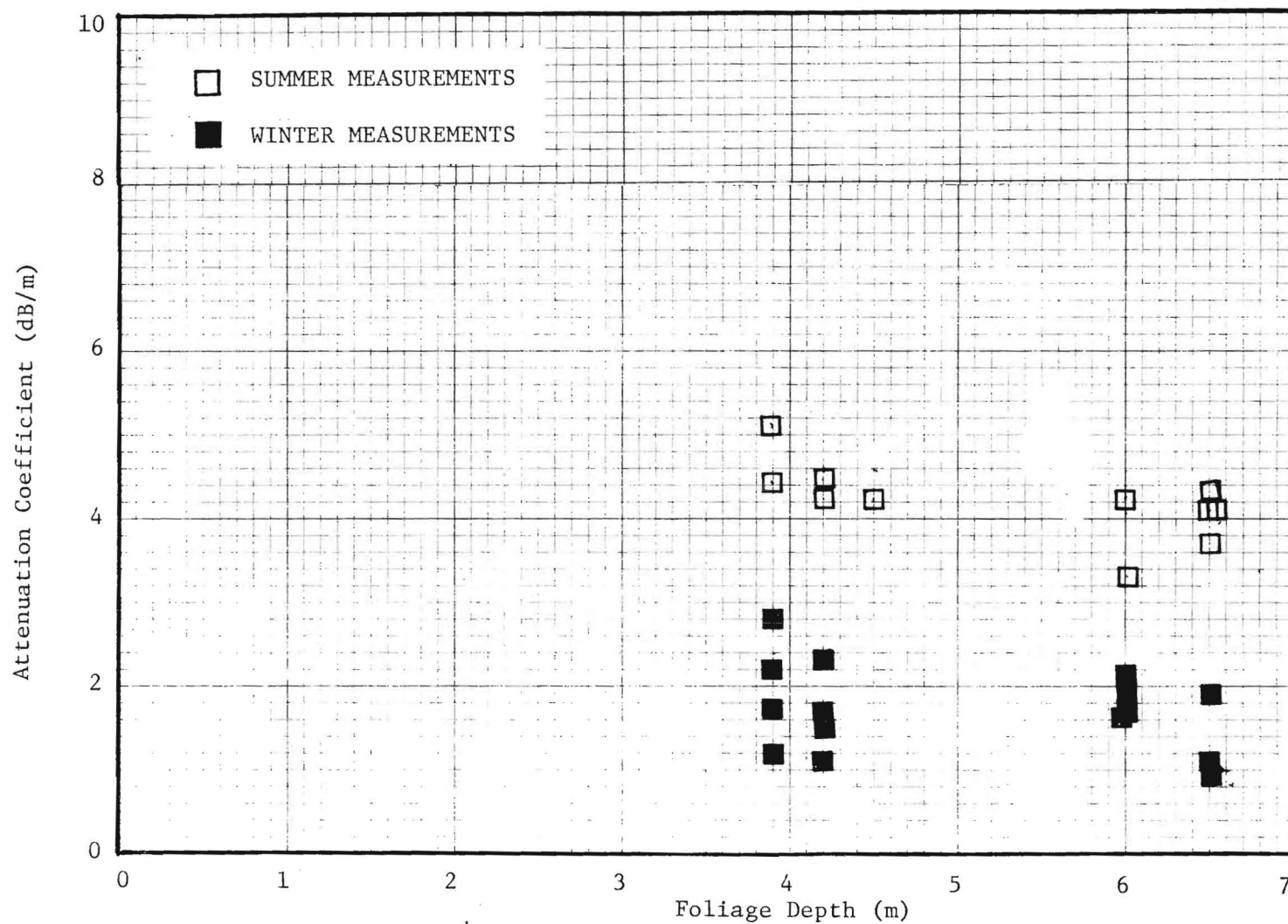


Figure 29. Comparison of the summer/winter values measured for the foliage attenuation coefficient of a water oak tree as a function of foliage depth, 16.2 GHz, 29° depression angle.

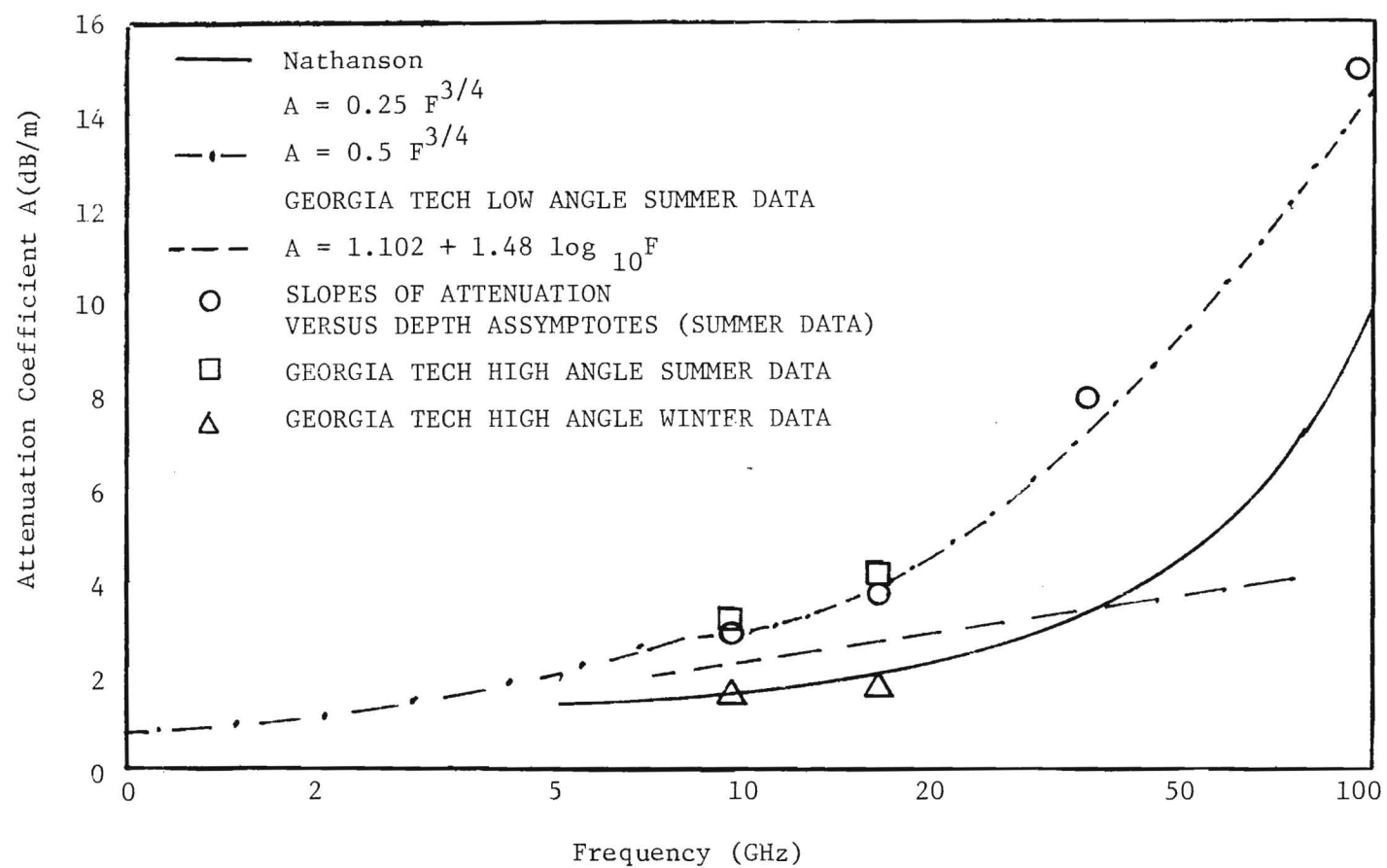


Figure 30. Summary of attenuation coefficient results for low-angle/high angle, summer/winter measurements as a function of frequency.

Probability that the Relative Power is Less than the Abcissa

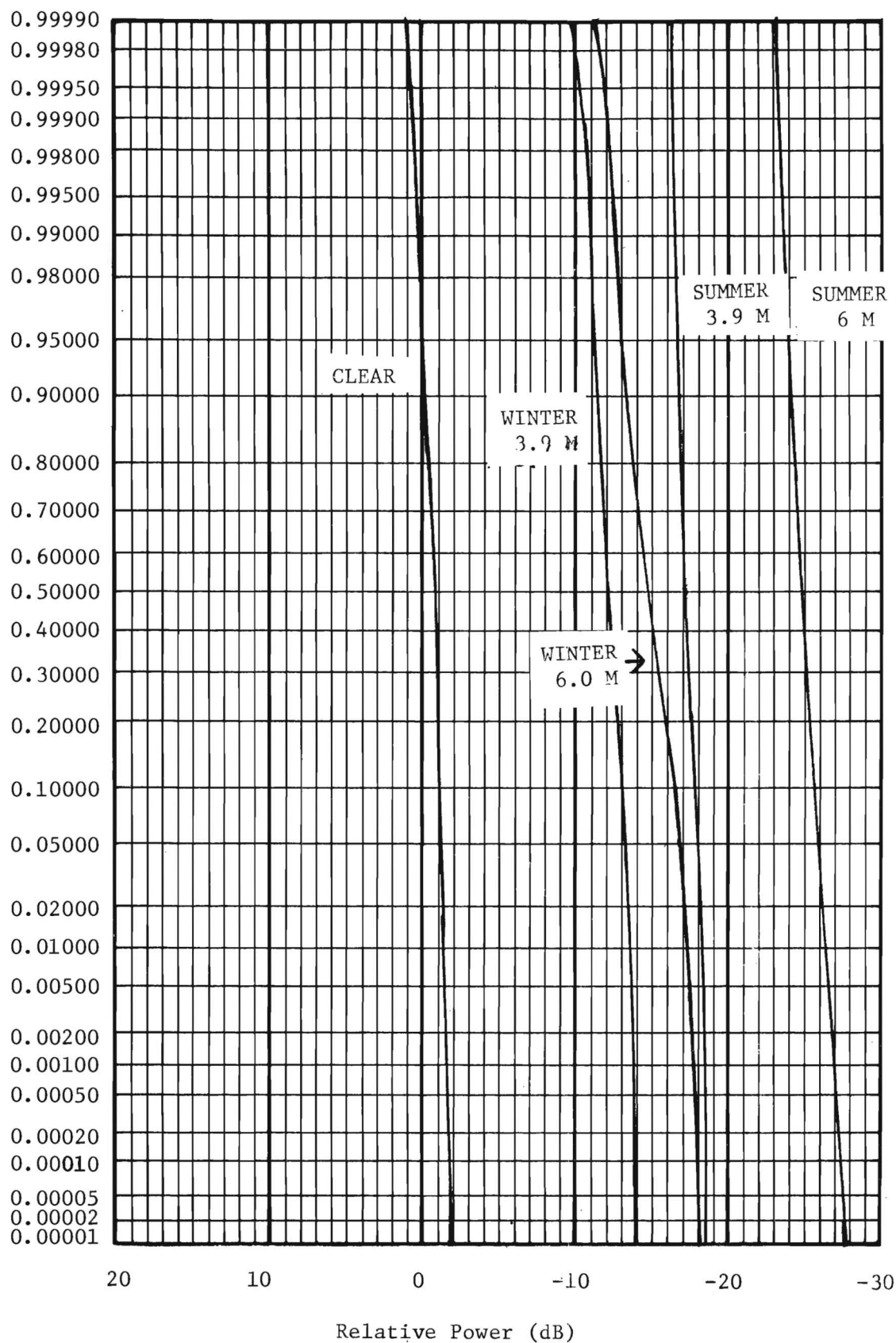


Figure 31. Probability distributions of the relative power received through a tree canopy for winter/summer foliage conditions and foliage depths of 3.9 m and 6.0 m, 9.4 GHz.

Probability that the Relative Power is Less than the Abscissa

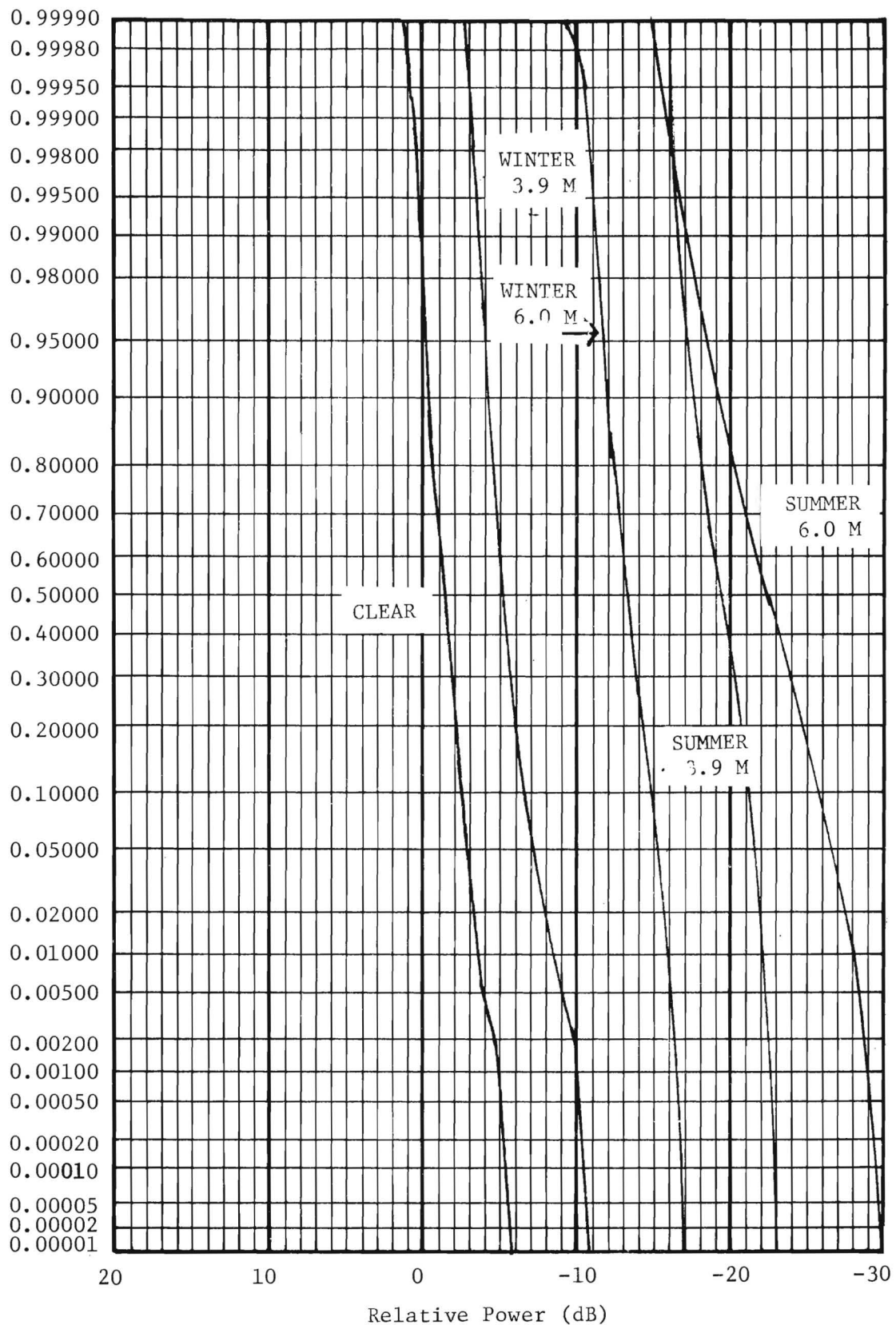


Figure 32. Probability distributions of the relative power received through a tree canopy for winter/summer foliage conditions and foliage depths of 3.9 m and 6.0 m, 16.2 GHz.

noted that the distribution widths increase with foliage depth and with frequency as would be expected. From the small amount of data available here, it appears that the tree limbs have a very large effect on the penetration properties of a tree canopy.

7. CONCLUSIONS AND RECOMMENDATIONS

The detailed discussions of the results of the investigations given in the preceding sections provide a fairly complete review of the experimental program. Unfortunately, only very limited analytical studies and no theoretical investigations were possible due to the fiscal constraints on the program. A number of significant conclusions have been determined and are outlined below.

1. Dry measurements indicate that the attenuation constant varies directly with the log of the frequency and is essentially independent of polarization.
2. Wet summer measurements indicate that the attenuation constant is a power function of the log of the frequency.
3. Dry winter measurements indicate that the attenuation constant is much less than for the summer (foliated) case. Insufficient data is available to determine the frequency dependence above Ku-Band.
4. The summer attenuation constant appears to increase with foliage depth, particularly at 35 GHz and 95 GHz for both horizontal and vertical polarizations. This effect was not observed for the winter (defoliated) measurements.
5. Two-way summer measurements at 35 GHz and 95 GHz were limited to 4 meters foliage depth or less. The apparent increase in attenuation constant with foliage depth indicates the possibility of higher average values of attenuation for greater foliage depths than those measured.
6. One-way summer measurements tended to give higher median values for the attenuation constant than the two-way measurements. The difference is attributed to differences in illumination functions and in foliage depths measured.
7. High-angle summer measurements gave larger values of attenuation constant than the low-angle measurements. The difference is attributed to greater density of branches and limbs for the high-angle case.
8. The winter high-angle measurements gave lower values than the summer values for the attenuation coefficient; however, the attenuations measured were significant indicating that limbs do affect the attenuations.

9. The probability distributions of the received signal exhibited little difference in width between the foliated and defoliated measurements indicating that variations in the attenuation are probably due to movements of limbs in and out of the beam path for both cases.

Perhaps one of the most important results of these investigations is the establishment of a potentially reproducible definition of foliage depth. The generally used definition of foliage depth appears to be a measure of total foliage path-length based on the line-of-sight distance through the canopy. Unfortunately, this approach requires a detailed description of the foliage (i.e., type of vegetation, density, etc.) and is not simply reproducible, especially in diverse geographic regions. The proposed definition which was used for the data presented here describes a total foliage depth based on the number of branches in the path and the size of each branch. This definition is applied to defoliated branches by assuming the branch size is equal to the gross diameter of the branch and twigs. This approach shows promise in developing prediction models and in providing a measurements standard, since a surprising degree of similarity in attenuation characteristics apparently exists between foliage types at a branch level.

The current work has really only barely begun the investigation of foliage penetration by the shorter microwave and millimeter wavelengths. A great deal of additional work is needed to provide a comprehensive base for the characterization of the penetration questions. A few specific items recommended are given below.

1. One-way penetration measurements should be performed for both winter and summer conditions at the higher depression angles for 1, 6, 10, 16, 35, and 95 GHz.
2. Additional two-way penetration measurements are needed for summer conditions with emphasis on moderate-to-large foliage depths.
3. The types of foliage encountered should be expanded by performing measurements at several sites.
4. Future experimental programs should include detailed characterization of the foliage and/or branches for the defoliated state, especially moisture content, leaf thickness and density, as well as more extensive meteorological documentation.

5. Extensive analytical and theoretical investigations should be undertaken to support and guide the experimental measurements.
6. The development of computer algorithms based on the results of the experimental and analytical investigations should be initiated.

REFERENCES

1. INFORMATION THEORY, Stanford Goldman, Prentice-Hall, Inc. (1953).
2. "Radar Tracking Accuracy Improvement by Means of Pulse-to-Pulse Frequency Agility," W. P. Birkmeier and N. D. Wallace, IEEE Transactions on Communication and Electronics AP, January 1963.
3. "The Origins of Radar Fluctuations," H. Goldstein, PROPAGATION OF SHORT RADIO WAVES, D. E. Kerr, Editor, MIT Radiation Laboratory Series, Volume 13, McGraw-Hill Book Company, Inc. (1951).
4. "Improving Radar Range and Angle Detection with Frequency Agility," H. K. Ray, 11th Annual East Coast Conference on Aerospace and Navigational Electronics, 21-23 October 1964, Baltimore, Maryland.
5. R. D. Hayes and F. B. Dyer, "Land Clutter Characteristics for Computer Modeling of Fire Control Radar Systems," Technical Report No. 1 on Contract DAAA-25-73-C-0256, Engineering Experiment Station, Georgia Institute of Technology, 15 May 1973.
6. N. C. Currie, F. B. Dyer, and R. D. Hayes, "Analysis of Radar Rain Return at Frequencies of 9.375, 35, 70, and 95 GHz," Technical Report No. 2 on Contract DAAA-25-73-C-0256, Engineering Experiment Station, Georgia Institute of Technology, 2 April 1975.
7. N. C. Currie, F. B. Dyer, and R. D. Hayes, "Radar Land Clutter Measurements at Frequencies of 9.5, 16, 35 and 95 GHz," Technical Report No. 3 on Contract DAA-25-73-C-0256, Engineering Experiment Station, Georgia Institute of Technology, 2 April 1975.
8. N. C. Currie, E. E. Martin, and F. B. Dyer, "Radar Foliage Penetration Measurements at Millimeter Wavelengths," Technical Report No. 4 on Contract DAAA-25-73-C-0256, Engineering Experiment Station, Georgia Institute of Technology, 31 December 1975.
9. Fred E. Nathanson, Radar Design Principles, McGraw-Hill Book Company, New York, 1969, p. 19.
10. J. A. Saxton and J. A. Lane, "VHF and UHF Reception, Effects of Trees and Other Obstacles," Wireless World, Vol. 61, May 1955, pp. 229-232.